NASA Technical Paper 1901

Simulation of Ideal-Gas Flow by Nitrogen and Other Selected Gases at Cryogenic Temperatures

Robert M. Hall and Jerry B. Adcock

SEPTEMBER 1981

NASA

NASA Technical Paper 1901

Simulation of Ideal-Gas Flow by Nitrogen and Other Selected Gases at Cryogenic Temperatures

Robert M. Hall and Jerry B. Adcock
Langley Research Center
Hampton, Virginia

NASA
National Aeronautics
and Space Administration

Scientific and Technical
Information Branch

1981

SUMMARY

Since transonic flight vehicles normally operate at temperatures and pressures for which the atmosphere behaves as an ideal diatomic gas, it is important for the test gas in a transonic cryogenic wind tunnel to act accordingly. Nitrogen is the most extensively used test gas in cryogenic tunnels. However, the thermodynamic properties of nitrogen gas deviate from those of an ideal diatomic gas at cryogenic temperatures. Choice of a suitable equation of state to model nitrogen's behavior is discussed, and the equation of Beattie and Bridgeman is selected as adequate for cryogenic wind tunnel use. The real-gas behavior of nitrogen is compared with an ideal diatomic gas for the following flow processes: isentropic expansions, normal shocks, boundary layers, and interactions between shock waves and boundary layers. The only differences in predicted pressure ratio between nitrogen and an ideal gas which may limit the minimum operating temperatures of transonic cryogenic wind tunnels occur at total pressures approaching 9 atm and total temperatures 10 K below the corresponding saturation temperature. These pressure differences approach 1 percent for both isentropic expansions and normal shocks.

Several alternative cryogenic test gases - dry air, helium, and hydrogen - are also analyzed. Differences between air and an ideal diatomic gas are similar to those for nitrogen and should present no difficulty. However, differences for helium and hydrogen are over an order of magnitude greater than those for nitrogen or air. It is concluded that helium and cryogenic hydrogen would not approximate the compressible flow of an ideal diatomic gas.

INTRODUCTION

Under normal conditions, cryogenic wind tunnels should be operated at the lowest possible total temperature in order to maximize Reynolds number capability for a given tunnel total pressure or to minimize costs of operating at a fixed Reynolds number. Not only does Reynolds number increase as the tunnel temperature decreases, but its rate of increase grows as well, as shown in figure 1, taken from reference 1. For operation at some Reynolds number below the maximum capability of the tunnel, testing at the lowest possible temperature maximizes the use of temperature reduction and minimizes the use of pressure increase to achieve the desired test Reynolds number. If pressure can be minimized, drive power, which is proportional to pressure, is minimized, and less liquid nitrogen (LN_2) is required for absorbing the heat added to the stream by the drive fan. Reductions in drive power and LN_2 usage lead to lower operational expenses. Operation at a reduced pressure also reduces the model loads and thus eases balance, sting, and model stress problems. The minimum operating temperatures are, however, limited by the low-temperature behavior of the test gas. At some temperature, either the test gas begins to condense or it does not simulate the nearly ideal-gas behavior of air encountered in transonic flight.

The present paper analyzes the thermodynamic properties of several cryogenic gases to determine whether they properly simulate an ideal diatomic gas, which is

defined for present purposes as being both thermally perfect (obeys ideal gas law) and calorically perfect (specific heats are constants with a ratio of 1.4). Although the greatest attention has been paid to nitrogen as a test gas for transonic cryogenic wind tunnels, other gases have been considered. For example, conversion of already existing ambient-temperature blowdown tunnels to cryogenic operation may be economically accomplished if dry air can be cooled by injecting liquid nitrogen directly into the tunnel flow. This process results in a test gas composed of a mixture of dry air and nitrogen. Also, since unit Reynolds number increases with decreasing temperature, gases with much lower boiling temperatures than nitrogen have been considered as a means of testing at higher unit Reynolds numbers at the same operating pressure. The alternative gases in this category include helium and hydrogen.

The emphasis of the present study is on the analysis of nitrogen because of the extensive use of nitrogen as the test gas. The study reviews the reasons to suspect nonideal behavior of nitrogen, summarizes and compares the available equations of state for modeling it, and examines its real-gas behavior for a variety of flow processes. Also, because of the interest in alternative test gases, air, helium, and hydrogen are briefly examined.

SYMBOLS

A_o, a, B_o, b, c	Beattie-Bridgeman constants, see equation (4)
c_p	specific heat at constant pressure, J/kg-K
c_v	specific heat at constant volume, J/kg-K
C_f	local skin friction coefficient, $\frac{\tau}{(1/2)\rho_\infty u_\infty^2}$
h	specific enthalpy, J/kg
M	Mach number
p	pressure, N/m^2 or atm (1 atm = 101.3 kPa)
p_o	reference pressure, Pa
R_x	Reynolds number based on position x
$\mathcal{R}$	specific gas constant, J/kg-K
s	specific entropy, J/kg-K
T	temperature, K
T_o	reference temperature, K
u	velocity, m/sec
v	specific volume, m^3/kg

x	distance from leading edge, m
y	vertical distance from surface, m
Z	compressibility factor, $pv/\mathcal{R}T$
γ	ratio of specific heats, c_p/c_v
δ	boundary-layer thickness, m
δ^*	boundary-layer displacement thickness, m
ζ	incident shock angle, deg
θ	boundary-layer momentum thickness, m
ρ	density, kg/m^3
τ	shear stress, N/m^2

Subscripts:

aw	adiabatic wall
t	total conditions
1	upstream of normal shock
2	downstream of normal shock
∞	free-stream conditions

Superscripts:

*	values at reference temperature and pressure
0	zero-pressure conditions

Abbreviations:

BB	Beattie-Bridgeman equation of state
NBS-NASA	equation of state developed by the National Bureau of Standards for NASA
ONSET	onset of condensation
SAT	saturation
VDW	Van der Waals equation of state

REAL-GAS PROPERTIES OF NITROGEN

The necessity of examining the real-gas behavior of nitrogen at low temperatures is obvious after graphing the compressibility factor Z and the ratio of specific heats γ as a function of temperature. Such graphs are shown in figures 2 and 3 for various equations of state, which are discussed later. As temperature decreases, both Z and γ depart significantly from the values associated with a thermally perfect ($Z = 1.0$) and a calorically perfect ($\gamma = 1.4$) diatomic gas. Since the goal of testing in a cryogenic tunnel is to simulate flight through the atmosphere at conditions for which $Z \approx 1.0$ and $\gamma \approx 1.4$, figures 2 and 3 suggest that a complete real-gas analysis of nitrogen is necessary to ensure the proper performance of nitrogen as a test gas.

EQUATIONS OF STATE

Before a complete analysis of nitrogen (or of alternative gases) can be performed, one must be able to characterize the behavior of the gas. The mathematical form of that characterization is called an equation of state, usually taking a form similar to

$$p = f(v,T) \tag{1}$$

where p is pressure and f is some arbitrary function of volume and temperature. The next section summarizes the various equations of state that are typically used to describe gases.

Equations Available

The simplest and most widely used equation in fluid mechanics is the ideal equation of state represented by

$$pv = RT \tag{2}$$

where R is the specific gas constant. The basic assumptions embodied in equation (2) are that the gas molecules do not attract each other and that the molecules themselves occupy no volume. The compressibility factor Z, which equals pv/RT, is obviously equal to 1.0, and the gas is consequently thermally perfect. That Z does not equal 1.0 and that γ is a function of pressure (ref. 2) as well as of temperature demonstrate the inability of the ideal equation of state to properly predict the thermodynamic properties of nitrogen at low temperatures. However, as shown later in this paper, these deviations do not necessarily affect the ability of nitrogen to simulate the flow processes of an ideal diatomic gas with $Z = 1.0$ and $\gamma = 1.4$.

Since the ideal equation of state does not adequately represent Z at low temperatures, an improved equation might be obtained by correcting for the assumptions in the ideal equation. The first step to improve the equation would be to incorporate the physical realities of attraction and finite volume into a more advanced equation of state. This was done successfully by J. D. Van der Waals in 1873, as described in detail by Glasstone in reference 3, pages 244-300. Attraction between

molecules requires a positive correction to measured gas pressure, and the finite volume of the molecules requires a negative correction for specific volume. Consequently, the Van der Waals equation of state is written as

$$\left(p + \frac{\alpha}{v^2}\right)(v - \beta) = RT \tag{3}$$

where α and β represent constants for a particular gas. Equation (3) is referred to in this paper as the VDW equation. While the VDW equation of state represented a substantial improvement over the ideal equation of state in its ability to model gases, equation-of-state development has continued up to the present.

The remaining equations of state to be discussed here are much more complicated but remain basically empirical. In 1927, Beattie and Bridgeman developed an equation of state that has proved to be very useful and accurate. The general form of the Beattie-Bridgeman equation (to be referred to as the BB equation) is given by

$$p = \frac{RT(1 - \varepsilon)}{v^2}(v + B) - \frac{A}{v^2} \tag{4}$$

where

$$A = A_o\left(1 - \frac{a}{v}\right)$$

$$B = B_o\left(1 - \frac{b}{v}\right)$$

$$\varepsilon = \frac{c}{vT^3}$$

and where A_o, a, B_o, b, and c are constants that are tabulated in reference 4 for many different gases. The values of these constants for nitrogen are given below after conversion to SI units:

$$A_o = 173.60 \text{ N-m}^4/\text{kg}^2$$

$$a = 0.0009342 \text{ m}^3/\text{kg}$$

$$B_o = 0.001801 \text{ m}^3/\text{kg}$$

$$b = -0.000247 \text{ m}^3/\text{kg}$$

$$c = 1499 \text{ m}^3\text{-K}^3/\text{kg}$$

The specific gas constant R is taken to be 296.79 J/kg-K.

One of the most complicated equations of state developed specifically for nitrogen is that reported by Jacobsen in reference 2. He used a 32-term equation that describes both liquid and gaseous phases of nitrogen. Jacobsen's equation can also be found in reference 5, which is a valuable reference because it contains tabular values of, or equations for, transport properties such as thermal conductivity and viscosity.

Because of the complexity and the wide range of applicability of Jacobsen's equation (pressures up to 10 000 atm and temperatures from 65 K to 2000 K), NASA Langley Research Center contracted with the National Bureau of Standards to develop an optimized virial equation of state which would focus on pressures only up to 10 atm and temperatures only up to 300 K. Furthermore, the equation of state was to calculate properties of only gaseous nitrogen. Full details of this work are included in reference 6. The form of this optimized virial equation of state is

$$p = RT\rho(1 + B\rho + C\rho^2) \tag{5}$$

where

$$B = \sum_{j=1}^{7} B_j T^{(3-j)/2}$$

$$C = \sum_{j=1}^{5} C_j T^{(1-j)/2}$$

and ρ is density. Values for the constants B_j and C_j can be found in reference 6. This equation of state, referred to as the NBS-NASA equation, is compared with the other equations in the following section.

Comparing the Equations for Nitrogen

To compare the predictions of the different equations of state for flow problems, expressions are required for enthalpy h, entropy s, heat capacities c_p and c_v, and sound speed a. Reference 7, a very helpful article, discusses the calculation of these and other thermodynamic properties. The following equations are taken from that reference with the exception of the expression for c_p, which contains a typographical error in reference 7:

$$h = h^*_{T_o} + \int_0^{\rho} \left[\frac{p}{\rho^2} - \frac{T}{\rho^2}\left(\frac{\partial p}{\partial T}\right)_\rho\right] d\rho + \frac{p - \rho RT}{\rho} + \int_{T_o}^{T} c_p^0 \, dT \tag{6}$$

$$s = s^*_{T_o} + \int_{T_o}^{T} \frac{c_p^0}{T} dT - R \ln\left(\frac{\rho RT}{p_o}\right) + \int_0^{\rho} \left[\frac{R}{\rho} - \frac{1}{\rho^2}\left(\frac{\partial p}{\partial T}\right)_\rho\right] d\rho \tag{7}$$

$$c_v = c_v^0 - \int_T \int_0^\rho \frac{T}{\rho^2}\left(\frac{\partial^2 p}{\partial T^2}\right)_\rho d\rho \tag{8}$$

$$c_p = c_v + T\left(\frac{\partial p}{\partial T}\right)_\rho^2 \left[\rho^2\left(\frac{\partial p}{\partial \rho}\right)_T\right]^{-1} \tag{9}$$

$$a = \left[\left(\frac{c_p}{c_v}\right)\left(\frac{\partial p}{\partial \rho}\right)_T\right]^{1/2} \tag{10}$$

where a variable before an integral sign denotes path of integration, $h^*_{T_o}$ and $s^*_{T_o}$ are enthalpy and entropy at the reference temperature and pressure, and c_p^0 and c_v^0 represent zero-pressure values of specific heats. Although real gases approach ideal-gas behavior at zero pressure, that is,

$$c_p^0 = \frac{\gamma R}{\gamma - 1} \tag{11}$$

$$c_v^0 = c_p^0 - R \tag{12}$$

the value of γ may still be a significant function of temperature for many gases. For nitrogen, an eight-term expression is given in reference 2 to approximate c_p^0 although experience at NASA Langley Research Center indicates that this complexity is not needed for cryogenic wind tunnel operating conditions. Also, absolute values of the constants $h^*_{T_o}$ and $s^*_{T_o}$ are not important for fluid mechanics problems because one is usually working only with differences in h or s, not with absolute values.

In the comparisons between the performance of the different equations of state, only nitrogen gas is considered. The eight-term expression for c_p^0 is used in Jacobsen's formulation, while the value of c_p^0 is taken to be $3.5R$ for the BB, VDW, and NBS-NASA equations of state. The value of $3.5R$ is calculated from equation (11) by making the accurate assumption that $\gamma = 1.4$ for zero-pressure nitrogen over the temperature range of interest (see ref. 2).

The comparisons of predicted nitrogen-gas thermodynamic properties (Z, γ, and c_p) are shown in figures 2, 3, and 4, for a pressure of 5 atm. For all three properties, the values predicted by the Jacobsen, BB, and NBS-NASA equations agree very well, while the values predicted by the VDW equation agree less well, especially at the lower temperatures. In the United States, Jacobsen's formulation has been accepted by the National Bureau of Standards as the best general description for nitrogen, so it is labeled as the standard in the figures. That the VDW equation is less accurate at the lower temperatures is not surprising because of its simplicity; however, it does indicate the basic departures from the ideal values.

Although Jacobsen is usually considered the standard by which to compare other equations, figures 2, 3, and 4 can be used to estimate the possible uncertainties in the formulations of Jacobsen, BB, and NBS-NASA. From figure 4, for example, at saturation temperature, there appears to be a difference of about 8 percent in the three predicted values of c_p. The large uncertainty in heat capacities is addressed at some length in reference 6, which predicts that the heat capacities from the NBS-NASA equation are accurate to within 2 percent and therefore must be more accurate than those from the BB or Jacobsen equations. Having not been able in our work to determine which formulation gives the most accurate heat capacities, we generally consider the uncertainty in c_p to be that due to the total spread in values, or about 8 percent.

The remainder of the comparison between the equations of state involves simulation of an isentropic expansion to a Mach number M of 1.5. The data are presented in a fashion similar to that of reference 8; the expansion ratios, for example p/p_t, from the real-gas prediction are divided by their ideal diatomic gas values. The predictions of pressure, temperature, and density ratios are shown in figure 5 for a total pressure p_t of 9 atm and for total temperatures T_t from 300 K down to the saturation temperature for nitrogen. (An accurate expression for the vapor-pressure curve is given in ref. 2; a good approximation is given in ref. 9.) Once again, the VDW equation does not agree very well with the other three equations. An interesting observation in figure 5 is the good agreement between the BB and the Jacobsen formulations. The maximum differences over the temperature range between the ratios from the BB and the Jacobsen formulations are 0.03 percent for the pressure ratio, 0.02 percent for the temperature ratio, and 0.14 percent for the density ratio, the only difference of any magnitude. Consequently, the BB formulation should be an excellent approximation to the very complex Jacobsen formulation over the temperature and pressure ranges of interest for cryogenic wind tunnels. Wagner and Schmidt also reached the same conclusion in reference 10. The new NBS-NASA equation, however, does not compare as well with the Jacobsen equation. The maximum differences between the ratios from the NBS-NASA and Jacobsen equations are 0.11 percent for pressure ratio, 0.41 percent for temperature ratio, and 0.13 percent for density ratio. The NBS-NASA equation predicts noticeably smaller temperature deviations from ideal.

The BB equation of state appears to be the best choice because it is relatively simple, only five arbitrary constants, and it compares very favorably with the complete Jacobsen formulation. The BB equation has the advantage over Jacobsen's equation in wind tunnel data reduction of being a gas-only description of nitrogen. Consequently, no special arrangements are needed in data reduction if local temperatures fall below the vapor-pressure temperature. The NBS-NASA equation of state may prove to be a more accurate description of the gas than the Jacobsen or BB equation, but this is not known yet. While the NBS-NASA equation was derived using sound speed data unavailable either to Beattie and Bridgeman or to Jacobsen, it is not obvious that the NBS-NASA equation actually fits this new sound speed data any better than the previous formulations, as seen in reference 6. Because of this uncertainty and the added complexity of the NBS-NASA equation, the BB equation is preferred. The VDW equation is a big improvement over the ideal equation of state but does not seem to warrant serious attention because the more accurate BB equation can be used almost as easily.

HYBRID REAL-IDEAL CALCULATIONS

Many investigators have done quick analyses of real-gas effects by substituting real-gas values of some parameter such as γ into equations derived on the assump-

tion of a constant value of γ. While this procedure is perhaps an understandable first step in studying real-gas effects, it is incorrect because equations such as that for the pressure ratio in an ideal isentropic expansion,

$$\frac{p}{p_t} = \left(1 + \frac{\gamma - 1}{2} M^2\right)^{-\gamma/(\gamma-1)} \tag{13}$$

are derived by assuming that the gas is thermally and calorically perfect. If the gas is not calorically perfect and c_p, c_v, and γ are functions of temperature, then equation (13) simply does not apply. In fact, any predictions of real-gas effects using real-gas values of parameters substituted into ideal equations are not only incorrect but can also be very misleading, as can be seen in figure 6, which is taken from reference 8. Substituting $\gamma = 1.565$, the real-gas value of γ at 8 atm and 120 K, into equation (13) leads to a predicted pressure deviation of about 6 percent at $M = 1.4$ instead of the 0.7-percent departure in the opposite direction predicted by the real-gas solution.

REAL-GAS EFFECTS FOR NITROGEN

With the knowledge that the Beattie-Bridgeman (BB) equation of state agrees well with the Jacobsen formulation, we now focus on the deviation of nitrogen from the behavior of an ideal diatomic gas for isentropic expansions, normal shocks, boundary layers, and interactions between shock waves and boundary layers. With the exception of those for isentropic expansions, the calculations shown are taken from other reports. Whether the BB or the Jacobsen equation was used depends on the source.

Isentropic Expansions

The examination of isentropic flow expansions is carried out with the BB equation of state and, as mentioned earlier, with ideal values assumed for the zero-pressure heat capacities, c_p^0 and c_v^0. The three total pressures considered are 1, 5, and 9 atm; and total temperatures are varied from 300 K to below saturation temperature. The actual minimum temperatures shown are based on the prediction of the onset of condensation effects due to homogeneous nucleation as reported by Sivier in reference 11. These minimum temperatures represent a probable lower temperature limit, since the flow at any lower temperature would have undergone spontaneous nucleation and would not be very useful as a test gas. Minimum operating temperature limits due to the onset of condensation effects are discussed in more detail in reference 12.

As in a previous section, the real-gas expansion ratios of pressure, temperature, and density are normalized by the comparable ideal-gas expansion ratio. These three ratios are shown in figure 7 as a function of total temperature at total pressures of 1, 5, and 9 atm for isentropic expansions to $M = 1.5$. The pressure ratios depart from ideal values by about 0.7 percent for 9 atm at the saturation temperature (labeled "SAT") and by nearly 1 percent at the total temperature corresponding to the possible onset of homogeneous nucleation (labeled "ONSET"). At the lower pressures of 5 and 1 atm, the maximum deviations are about 0.6 and 0.2 percent before the onset of nucleation. Very similar magnitudes at low temperatures are shown for the deviation in temperature ratio in figure 7(b); however, deviations at 300 K approach

0.2 percent for 9 atm and 0.1 percent for 5 atm. The density expansion ratios, shown in figure 7(c), display behavior somewhat different from the pressure or temperature ratios. First, at 300 K, deviations at 9 and 5 atm are 0.5 and 0.3 percent, respectively; and second, deviations at the low-temperature boundary do not smoothly increase with pressure. At the temperatures predicted for the onset of homogeneous nucleation, density ratio deviations for 1, 5, and 9 atm are, respectively, 0.3, 0.6, and 0.5 percent.

The deviations from ideal diatomic gas values for isentropic expansions do not appear to be of a magnitude to be of concern except perhaps at 9 atm below the saturation temperature. At these conditions, pressure may deviate by as much as 1 percent, and a data correction procedure may be appropriate in conjunction with a real-gas formulation. A more complete description of the isentropic expansion process is included in reference 8. Since the Jacobsen formulation treats nitrogen as a liquid at temperatures below the vapor-pressure curve, the study in reference 8 was limited to temperatures above saturation.

Normal Shocks

For normal shocks, ratios of various quantities across the shock are normalized by the ratios for an ideal diatomic gas. The results are taken from reference 8, which used the Jacobsen formulation, and are calculated down to the appropriate saturation temperature. Upstream and downstream quantities are subscripted by 1 and 2, respectively.

The differences in the ratios of static pressure, temperature, and density across the normal shock are shown in figure 8 for an upstream total pressure of 8 atm, upstream total temperatures from 300 K down to saturation temperature, and upstream Mach numbers of 1.4, 1.7, and 2.0. (Ref. 8 includes further figures showing that the effects of pressure are roughly proportional to the operating pressure. In other words, effects at 4 atm would be approximately half of those shown in the present example of 8 atm.) As seen in figure 8(a), the greatest deviation in pressure ratio between real and ideal flow, a value of about 0.6 percent at saturation temperature, occurs at $M_1 = 1.7$. The deviations in static-temperature ratio (fig. 8(b)) reach about 0.5 percent at $M_1 = 2.0$, and deviations in static-density ratios (fig. 8(c)) reach a maximum of about 0.4 percent at 250 K for $M_1 = 2.0$.

The ratios of total pressure, temperature, and density across the normal shock are shown in figure 9 for the same upstream Mach numbers and a total pressure of 8 atm. A maximum deviation of 0.2 percent in the total-pressure ratio occurs at about 275 K for $M_1 = 2.0$. The maximum total-temperature-ratio deviation is about 1.4 percent at saturation temperature for $M_1 = 2.0$. A maximum deviation in total-density ratio of about 0.3 percent occurs near room temperature for $M_1 = 2.0$.

The last figure in this series, figure 10, shows the ratio of the real to the ideal downstream Mach number M_2 as a function of total temperature for an upstream Mach number M_1 of 2.0 and a total pressure of 10 atm. The maximum departure from the ideal value is only 0.1 percent for this severe high-pressure case.

Cryogenic nitrogen gas appears to adequately simulate ideal diatomic normal shock flow. Deviations in the static-pressure ratio reach 0.6 percent at the saturation temperature for a total pressure of 8 atm. If operation at 9 atm and 10 K below saturation (corresponding to the predicted onset of homogeneous nucleation) is desired, this deviation could increase to about 0.9 percent. The departures in

static temperature are of the same magnitude as those for pressure, while departures in static density appear to be less. The departures of the ratios of total pressure and density are not significant, but there are relatively large deviations in the ratio of total temperatures. A deviation in this quantity is not considered significant for most data of transonic interest because heat transfer is not normally significant. None of the above differences appear to influence the downstream value of Mach number.

An additional comment should be made before leaving normal shock flows. In showing real-gas effects for shock flows, some authors have chosen to calculate

$$\% \text{ Difference} = \frac{\rho_{2,\text{real}} - \rho_{2,\text{ideal}}}{\rho_{2,\text{ideal}}} \times 100 \tag{14}$$

for given static values of upstream pressure p_1 and temperature T_1. The problem with this approach is that by specifying p_1 and T_1 for both the ideal and the real case, very different values of ρ_1 are required because of the compressibility Z of nitrogen shown in figure 2. For example, for upstream static conditions of 5 atm and 120 K, figure 2 implies a difference in density ρ_1 of 6 percent between the ideal-gas value and the Jacobsen value. Consequently, even if the ρ_2/ρ_1 ratios for the ideal and real shock flows were identical, equation (14) would still suggest a difference of 6 percent. Instead of being an indicator of the real-gas behavior of nitrogen through a shock, equations like (14) may be showing only the influence of a parameter such as compressibility.

Boundary Layers on Flat Plates

The next major flow process discussed is boundary-layer simulation over a flat plate. This section draws from work in reference 13 that utilized the Jacobsen formulation for the equation of state. As discussed in reference 13, in boundary-layer calculations, not only is the equation of state important, but also the expression for viscosity. The expression for the viscosity of nitrogen used in this analysis comes from reference 5 and includes a total of nine constants in a low-density term and seven additional constants in what is called a dense-fluid contribution. (The equation and accompanying constants are also described and discussed in ref. 8.) The real-gas parameters to be examined in this section include boundary-layer displacement thickness δ^*, boundary-layer thickness δ, skin friction coefficient C_f, and boundary-layer momentum thickness θ, for laminar and turbulent adiabatic-wall boundary layers. Also shown are the real-to-ideal ratios for quantities inside the boundary layer such as T, h, h_t, and ρ.

The parameters δ^*, δ, C_f, and θ for laminar adiabatic-wall boundary layers on a flat plate are summarized in figure 11 where they are shown normalized by values calculated for an ideal diatomic gas at 1 atm and 300 K with viscosity represented by Sutherland's formula. Figure 11(a) shows these parameters as a function of total pressure, and, surprisingly, the maximum deviation in δ^* from the ideal value occurs at the lowest total pressure. This unexpected result, explained in detail in reference 13, is caused by two compensating effects: the real-gas imperfections of nitrogen and the change with increasing pressure in the slope of viscosity as a function of temperature. (This observation was made earlier by Wagner and Schmidt in ref. 10.) The same four parameters are shown as a function of free-stream Mach num-

ber M_∞ in figure 11(b). Real-gas effects generally increase with increasing M_∞. The deviation for δ^* is about 1.3 percent for $M_\infty = 2.0$, $p_t = 9$ atm, and $T_t = 150$ K. Similar trends are found in figure 12 for turbulent adiabatic-wall boundary layers on a flat plate except that the magnitudes of the deviations are generally less than those for laminar boundary layers. (An assumption is made in the turbulent calculations that the turbulence model remains valid over the temperature range. As shown later, this appears to be a good assumption.)

Next, ratios of quantities inside the boundary layer are summarized for both laminar and turbulent boundary-layer profiles. The results for the laminar boundary layer are shown in figure 13(a). The velocity ratio is not shown because the agreement is so good that the ratio does not differ from the value of 1.0 to the scale of this plot. The only large deviation, 2 percent, occurs for static temperature but does not appear to be of consequence according to reference 13, since the primary boundary-layer quantities such as δ^*, δ, C_f, θ, and velocity are not affected. The similar plot for the turbulent boundary layer is shown in figure 13(b). The agreement here is generally better than in the laminar case except for the temperature ratio. In this figure, velocity and total enthalpy are not plotted because of their excellent agreement with ideal values. Again, no significance was attached to the temperature differences.

Although the flat-plate analysis found little reason for concern about adequate boundary-layer simulation, the differences between the predicted adiabatic-wall temperatures for cryogenic nitrogen and those for an ideal diatomic gas appeared to be large enough to be verifiable by experiment. Consequently, a two-dimensional airfoil instrumented with thermocouples for measuring surface temperature was tested in the Langley 0.3-Meter Transonic Cryogenic Tunnel (ref. 14). A sample of the results is given in figure 14. At 299 K, the wall temperatures are essentially those anticipated for the ideal gas. However, as the total temperature is reduced, the wall temperatures are lower than those for the ideal gas, as would be expected from the temperature profiles shown in figure 13. The magnitude of the adiabatic-wall temperature decrease is well predicted by the theory; this agreement adds greatly to the confidence level in this theoretical boundary-layer analysis and particularly to the applicability of the turbulence model used in reference 13 to cryogenic temperatures.

Interactions Between Shock Waves and Boundary Layers

In this section the real-gas behavior of nitrogen in an interaction between a shock wave and a laminar boundary layer is analyzed. The results presented have been calculated by Wagner and Schmidt in reference 10 using the BB equation of state for nitrogen and a numerical program with a fine mesh description of the boundary-layer region and a coarse mesh description of the outer inviscid flow field. As a demonstration of the accuracy of the program, results from the ideal equation of state are compared with experimental data of Hakkinen et al. (ref. 15) in figures 15 and 16 for an incident shock angle ζ of 32.6°. Wagner and Schmidt then make real-gas calculations for upstream static conditions of $p_\infty = 1$ bar and $T_\infty = 78$ K, where 1 bar = 0.987 atm. The static conditions are at the saturation temperature for nitrogen and correspond to total conditions of 7.7 atm and 140 K. As shown in figure 15, the magnitude of differences between the ideal and real values of p/p_∞ is less than 0.4 percent and would seem to be quite acceptable given the total conditions of 7.7 atm and 140 K. It is interesting to note, as Wagner and Schmidt do, that the real-gas deviations of pressure in the boundary layers (shown by the shaded area) correspond to the deviations of static pressure in the outer inviscid flow

(shown by the dashed line). The skin friction coefficient and the calculated differences between real- and ideal-gas values are shown in figure 16. The maximum differences in skin friction coefficient seem to be on the order of 5 percent, although it is not clear how much is due to numerical error. (Further work on skin friction may be desirable.) Given the good pressure agreement and fair agreement in skin friction coefficient, this flow process should not pose a problem for testing in cryogenic nitrogen.

Summary of Nitrogen Analysis

The study of cryogenic nitrogen as a wind tunnel test gas has indicated the following results. As shown by both the isentropic expansion analyses and the normal shock analyses, pressure ratios depart from ideal diatomic gas behavior by more than 0.5 percent only at pressures greater than 5 atm combined with temperatures near or below saturation. With a total pressure of 9 atm and total temperatures below saturation, the pressure ratios may be in error by about 1 percent. If accuracy greater than this is required, either temperatures below saturation must be avoided at high pressures or procedures must be devised to correct the data. The boundary-layer analyses also show effects in displacement thickness as large as 1.3 percent for $p_t = 9$ atm and $M = 2.0$. At low temperatures and high pressures, the Reynolds number should be very large, and the size of boundary layers about test models should be small compared with the thickness of the model. Consequently, the change in displacement thickness of 1.3 percent may not significantly affect the data because of the small size of the original boundary layer. The difference of 2 percent in temperature profile through the boundary layer does not seem to affect other quantities and is not considered significant. Wagner and Schmidt's analysis of interactions between shock waves and laminar boundary layers shows possible differences in C_f of about 5 percent. Because there is uncertainty in the magnitude of numerical scatter in their calculation, further analysis may be worthwhile.

ALTERNATIVE CRYOGENIC GASES

Although nitrogen is normally used as a test gas for transonic cryogenic tunnels, other gases are either being used or being considered as alternatives to nitrogen. In cryogenic blowdown facilities such as those of McDonnell-Douglas in California, dry air is cooled to cryogenic temperatures by injecting an almost equal mass of liquid nitrogen; consequently, the test gas is a mixture of dry air and nitrogen. To approximate the behavior of this mixture, an isentropic expansion and a normal shock were modeled by the Beattie-Bridgeman (BB) equation of state with appropriate constants for air. (The actual behavior of the mixture of dry air and nitrogen would be expected to be between the individual behavior of the two.) Further interest has also surfaced from time to time in using gases that have significantly lower liquefaction temperatures than nitrogen in order to test at larger unit Reynolds number. Helium and hydrogen are considered because at 1 atm, helium boils at 4.3 K and hydrogen at 20.4 K. Helium is also examined using the BB equation of state, but because of some thermodynamic anomalies to be explained later, hydrogen requires additional attention.

Air

The first alternative gas to be discussed is dry air. Since air is approximately 80 percent nitrogen, air and pure nitrogen would be expected to have very

similar properties. To see whether this is true or not, the isentropic expansion and normal shock ratios of pressure, temperature, and density have been evaluated for air and normalized by the ideal diatomic gas values ($Z = 1.0$ and $\gamma = 1.4$), as in figures 7 and 8. The constants used in the BB equation of state for air, found in reference 4, are given below in SI units:

$$A_o = 157.16 \text{ N-m}^4/\text{kg}^2$$

$$a = 0.0006666 \text{ m}^3/\text{kg}$$

$$B_o = 0.001592 \text{ m}^3/\text{kg}$$

$$b = -0.0003801 \text{ m}^3/\text{kg}$$

$$c = 1498 \text{ m}^3\text{-K}^3/\text{kg}$$

(These constants were in error in ref. 16.) The specific gas constant R is taken as 287.07 J/kg-K. The corresponding graphs for isentropic expansions in air are shown in figure 17, where the values are plotted from 300 K down to saturation temperature. As can be seen by comparing the pressure ratios in figures 17 and 7, there are virtually no differences between the real-gas performance of nitrogen and of air. Similarly, there are only small differences between the temperature and density ratios for nitrogen and air. The air results are plotted only down to saturation temperatures because, as explained in reference 12, air is not expected to undergo much cooling below saturation before the onset of condensation effects. The graphs for normal shock flows in air are shown in figure 18. Again the results for air are very similar to those for nitrogen in figure 8. On the basis of this brief examination, air would appear to be an acceptable cryogenic test gas. Consequently, using half air and half evaporated liquid nitrogen in a wind tunnel should present no difficulties, because the real-gas deviations should be somewhere between those predicted for pure nitrogen and those predicted for air. (The reason nitrogen is preferred to air for continuous flow fan-driven tunnels injecting a liquid cryogen for cooling is the availability of liquid nitrogen, the safety of using liquid nitrogen over using liquid air, and the lower saturation temperatures associated with pure nitrogen.)

Helium

As a first candidate for cryogenic operation at temperatures much colder than are possible for nitrogen, the monatomic gas helium is examined by using the following constants from reference 4 in the BB equation:

$$A_o = 137 \text{ N-m}^4/\text{kg}^2$$

$$a = 0.01495 \text{ m}^3/\text{kg}$$

$$B_o = 0.003498 \text{ m}^3/\text{kg}$$

$$b = 0$$

$$c = 10 \text{ m}^3\text{-K}^3/\text{kg}$$

(These constants were in error in ref. 16.) The specific gas constant R is taken to be 2077.3 J/kg-K. The results of the analysis are shown in figure 19; isentropic expansion ratios for pressure, temperature, and density normalized by the corresponding ideal diatomic gas ratios are shown as a function of Mach number M for two sets of total conditions. The first set is a total pressure of 1 atm and a total temperature of 300 K, at which helium acts like an ideal monatomic gas with $\gamma = 1.67$. The second set is a total pressure of 9 atm and a total temperature of 30 K and should be indicative of real-gas pressure and temperature effects. (The deviations are primarily due to decreased temperature rather than to increased pressure.) As is easily seen in all three ratios, the real-gas effects in helium due to increased pressure or reduced temperature are insignificant compared with the fundamental differences between monatomic helium with $\gamma = 1.67$ and an ideal diatomic gas with $\gamma = 1.40$. The pressure ratio differs from an ideal diatomic value by about 6 percent at $M = 2.0$ after passing through a maximum deviation of about 10 percent at $M = 1.4$. The temperature and density ratios show maximum deviations of about 23 and 26 percent at $M = 2.0$. These deviations from ideal diatomic gas behavior are over an order of magnitude larger than those calculated for nitrogen or air. In addition, since the pressure ratio shows a deviation of more than 1 percent at $M = 0.3$, the usefulness of helium as a transonic test gas would have to be seriously questioned, although there may be applications for helium in very low-speed flow situations that are often appropriate for industrial aerodynamics.

Hydrogen

Since helium does not appear to be useful as a transonic test gas, attention may be turned to hydrogen because of its low boiling temperature compared with nitrogen and because hydrogen, like air and nitrogen, is a diatomic gas. Hydrogen, however, is somewhat unusual because it has a nuclear spin anomaly. As explained in reference 17, the spin can be either parallel (orthohydrogen) or antiparallel (parahydrogen). At very low temperatures, an equilibrium mixture of orthohydrogen and parahydrogen is nearly all parahydrogen. At room temperature and above, the equilibrium concentrations approach those of so-called "normal" hydrogen, which is approximately 25 percent parahydrogen and 75 percent orthohydrogen. Furthermore, the rate of change of the concentrations is so slow at room temperatures and below that the half-life is measured in days if no catalyst is present. Consequently, it would be unlikely during an experiment that the percentages of orthohydrogen and parahydrogen would change unless a catalyst is introduced.

In most cryogenic concepts, the test gas is formed by evaporation from the liquid state, which for hydrogen would result in gaseous parahydrogen. In reference 18, Haut analyzed parahydrogen by using a polynomial interpolation equation of state. The pressure, temperature, and density ratios as calculated in reference 18 for an isentropic expansion to $M = 1.0$ are shown in figure 20. As is readily apparent, parahydrogen does not appear to simulate ideal diatomic flow. At low temperatures, the deviations in pressure ratio are approximately 8 percent, the deviations in temperature ratio are about 10 percent, and the deviations in density ratio are somewhat less, about 4 percent.

Rather than cooling the tunnel through injection of the test gas in the liquid state, one might use a heat exchanger to cool normal hydrogen (n-hydrogen) from ambient to cryogenic temperatures; then an analysis of the low-temperature behavior may be made with the BB constants for hydrogen from reference 4:

$A_o = 4924\ N\text{-}m^4/kg^2$

$a = -0.00251\ m^3/kg$

$B_o = 0.01040\ m^3/kg$

$b = -0.02162\ m^3/kg$

$c = 250\ m^3\text{-}K^3/kg$

The specific gas constant R is taken to be 4124.3 J/kg-K and values for the zero-pressure heat capacity can be taken from reference 17. Some uncertainty exists, however, in choosing the values of zero-pressure heat capacity, since the data used in determining the BB constants for hydrogen were taken before 1929, which was the year in which the two forms of hydrogen, parahydrogen and orthohydrogen, were shown to exist. Consequently, the low-temperature data used by Beattie and Bridgeman would be for n-hydrogen if the experiments were conducted before the concentrations of orthohydrogen and parahydrogen could approach their equilibrium values; or they would be for equilibrium concentration hydrogen (e-hydrogen) if a catalyst was present or if the hydrogen was kept cold for a relatively long period of time, hours or perhaps days. (Of course, the data may apply to some combination of e- and n-hydrogen.) Assuming that the BB constants are appropriate for n-hydrogen and using the corresponding n-hydrogen values for zero-pressure heat capacity, one obtains the behavior of n-hydrogen as represented in figure 21. If the assumption that the BB equation applies to n-hydrogen is correct, then n-hydrogen would not be very useful as a transonic test gas at cryogenic temperatures because of the large differences between the predicted ratios of static pressure, temperature, and density and those of an ideal diatomic gas. Assuming that the BB constants are appropriate for e-hydrogen and using the equilibrium values of zero-pressure heat capacity from reference 17, one obtains the behavior of e-hydrogen as shown in figure 22. If indeed the BB equation applies to e-hydrogen, then the magnitude of the differences between an ideal diatomic gas is smaller than for the assumed n-hydrogen example. However, it must be remembered that the molecular weight of hydrogen is much smaller than that of nitrogen and that this significantly reduces the Reynolds number. According to reference 19, the total temperature of hydrogen must be below 40 K before any Reynolds number advantage over nitrogen at the same pressure occurs. The 20-percent increase in Reynolds number (ref. 19) realized by using e-hydrogen at $T_t = 35$ K, where differences seem to be minimal, would not appear to be worthwhile, considering the safety risks of using hydrogen that are mentioned in reference 18.

CONCLUDING REMARKS

In transonic cryogenic wind tunnels, the test gas, usually nitrogen, must simulate an ideal diatomic gas, since transonic flight vehicles normally operate at conditions for which the atmosphere behaves as an ideal diatomic gas. It is necessary to be aware that at low temperatures, the behavior of nitrogen, as well as of other possible test gases, departs from ideal values for thermodynamic properties such as compressibility Z and ratio of specific heats γ. However, as shown in this paper and in several references, the deviations in Z and γ do not necessarily diminish the ability of nitrogen to simulate flow of an ideal diatomic gas with $Z = 1.0$ and $\gamma = 1.4$. To examine the simulation qualities of nitrogen, a complete real-gas analysis must be done. Substituting real values of Z and γ into ideal

equations derived with the assumption that Z and γ are constant is incorrect and can give very misleading indications of real-gas effects. When a complete real-gas analysis is done for nitrogen, only small differences are seen between nitrogen and an ideal diatomic gas for isentropic expansions, normal shocks, boundary layers, and interactions between shock waves and boundary layers. In fact, the only minimum operating temperature restriction that these real-gas effects may impose occurs at operating total pressures of about 9 atm, for which the pressure ratio deviations from ideal are as large as 1 percent if the total temperature is 10 K below saturation. If this deviation is too large, the total temperatures at pressures near 9 atm may have to be restricted to saturation temperature or above for wind tunnel operation.

Alternative gases have also been briefly investigated. Air appears to be comparable to nitrogen in simulating an ideal diatomic gas; consequently, minimum operating temperatures should not be limited by the behavior of gaseous air except, as in the case of nitrogen, perhaps at total pressures approaching 9 atm and at saturation temperatures. On the other hand, monatomic helium and the various nuclear forms of cryogenic hydrogen do not satisfactorily simulate compressible ideal diatomic flow. In general, they would not make good transonic test gases.

Langley Research Center
National Aeronautics and Space Administration
Hampton, VA 23665
July 31, 1981

REFERENCES

1. Kilgore, Robert A.; Adcock, Jerry B.; and Ray, Edward J.: Flight Simulation Characteristics of the Langley High Reynolds Number Cryogenic Transonic Tunnel. J. Aircr., vol. 11, no. 10, Oct. 1974, pp. 593-600.

2. Jacobsen, Richard T.: The Thermodynamic Properties of Nitrogen From 65 to 2000 K With Pressures to 10,000 Atmospheres. Ph. D. Thesis, Washington State Univ., 1972. (Available as NASA CR-128526.)

3. Glasstone, Samuel: Textbook of Physical Chemistry, Second ed. D. Van Nostrand Co., Inc., c.1946, pp. 244-300.

4. Beattie, James A.; and Bridgeman, Oscar C.: A New Equation of State for Fluids. II. Application to Helium, Neon, Argon, Hydrogen, Nitrogen, Oxygen, Air and Methane. J. American Chem. Soc., vol. 50, no. 12, Dec. 1928, pp. 3133-3138.

5. Jacobsen, R. T.; Stewart, R. B.; McCarty, R. D.; and Hanley, H. J. M.: Thermophysical Properties of Nitrogen From the Fusion Line to 3500 R (1944 K) for Pressures to 150 000 psia (10 342 × 10^5 N/m^2). NBS Tech. Note 648, U.S. Dep. Commer., Dec. 1973.

6. Younglove, Ben; and McCarty, R. D.: Thermodynamic Properties of Nitrogen Gas Derived From Measurements of Sound Speed. NASA RP-1051, 1979.

7. McCarty, R. D.: Determination of Thermodynamic Properties From the Experimental p-V-T Relationships. Experimental Thermodynamics. Volume 2 - Experimental Thermodynamics of Non-Reacting Fluids, Butterworth & Co., Ltd., c.1975, pp. 501-526.

8. Adcock, Jerry B.: Real-Gas Effects Associated With One-Dimensional Transonic Flow of Cryogenic Nitrogen. NASA TN D-8274, 1976.

9. Dodge, Barnett F.; and Davis, Harvey N.: Vapor Pressure of Liquid Oxygen and Nitrogen. J. American Chem. Soc., vol. 49, Mar. 1927, pp. 610-620.

10. Wagner, Bernhard; and Schmidt, Wolfgang: Theoretical Investigations of Real Gas Effects in Cryogenic Wind Tunnels. AIAA J., vol. 16, no. 6, June 1978, pp. 580-586.

11. Sivier, Kenneth R.: Digital Computer Studies of Condensation in Expanding One-Component Flows. ARL 65-234, U.S. Air Force, Nov. 1965. (Available from DTIC as AD 628 543.)

12. Hall, Robert M.: Real Gas Effects - II: Influence of Condensation on Minimum Operating Temperatures of Cryogenic Wind Tunnels. Cryogenic Wind Tunnels, AGARD-LS-111, May 1980, pp. 7-1 - 7-21.

13. Adcock, Jerry B.; and Johnson, Charles B.: A Theoretical Analysis of Simulated Transonic Boundary Layers in Cryogenic-Nitrogen Wind Tunnels. NASA TP-1631, 1980.

14. Johnson, Charles B.; and Adcock, Jerry B.: Measurement of Recovery Temperature on an Airfoil in the Langley 0.3-m Transonic Cryogenic Tunnel. AIAA-81-1062, June 1981.

15. Hakkinen, Raimo Jaakko; Greber, Isaac; Trilling, Leon; and Abarbanel, S. S.: The Interaction of an Oblique Shock Wave With a Laminar Boundary Layer. NASA MEMO 2-18-59W, 1959.

16. Hall, Robert M.: Real-Gas Effects I - Simulation of Ideal Gas Flow by Cryogenic Nitrogen and Other Selected Gases. Cryogenic Wind Tunnels, AGARD-LS-111, May 1980, pp. 5-1 - 5-16.

17. Farkas, Adalbert: Orthohydrogen, Parahydrogen and Heavy Hydrogen. Cambridge Univ. Press, 1935.

18. Haut, Richard C.: Evaluation of Hydrogen as a Cryogenic Wind Tunnel Test Gas. NASA CR-145186, 1977.

19. Goodyer, M. J.: The Principles and Applications of Cryogenic Wind Tunnels. Cryogenic Wind Tunnels, AGARD-LS-111, July 1980, pp. 1-1 - 1-6.

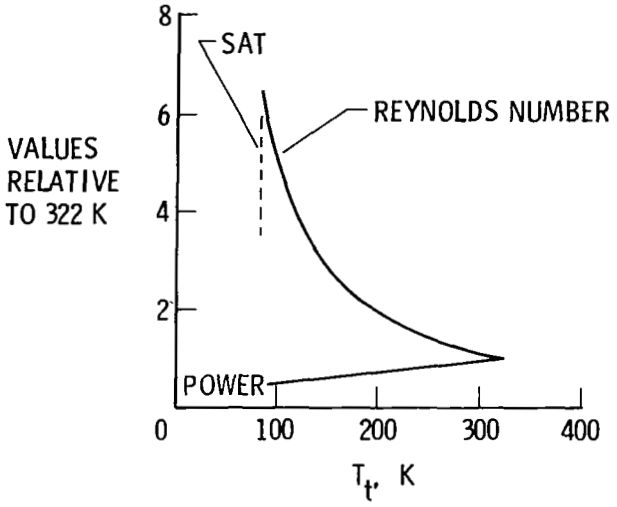

Figure 1.- Effect of temperature reduction on unit Reynolds number and drive power. Nitrogen gas; $M_\infty = 1.0$; $p_t = 1$ atm. (From ref. 1.)

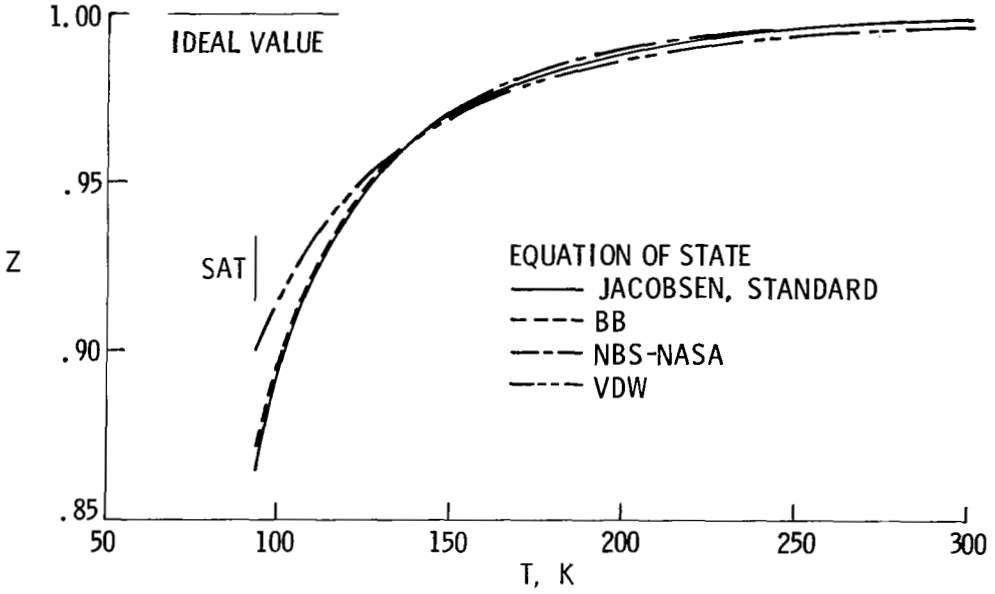

Figure 2.- Compressibility Z for nitrogen gas at p = 5 atm. The Jacobsen curve is taken to be the accepted value.

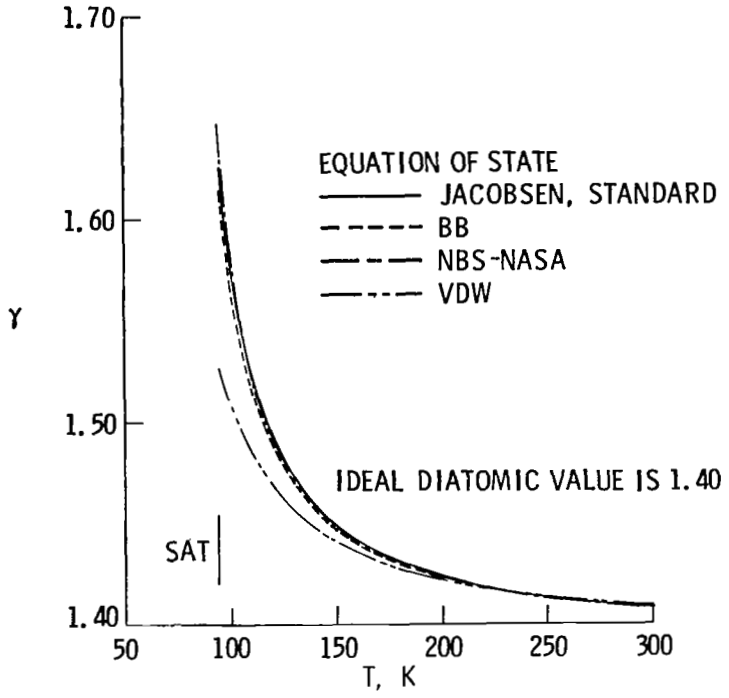

Figure 3.- Ratio of specific heats γ for nitrogen gas at $p = 5$ atm. The Jacobsen curve is taken to be the accepted value.

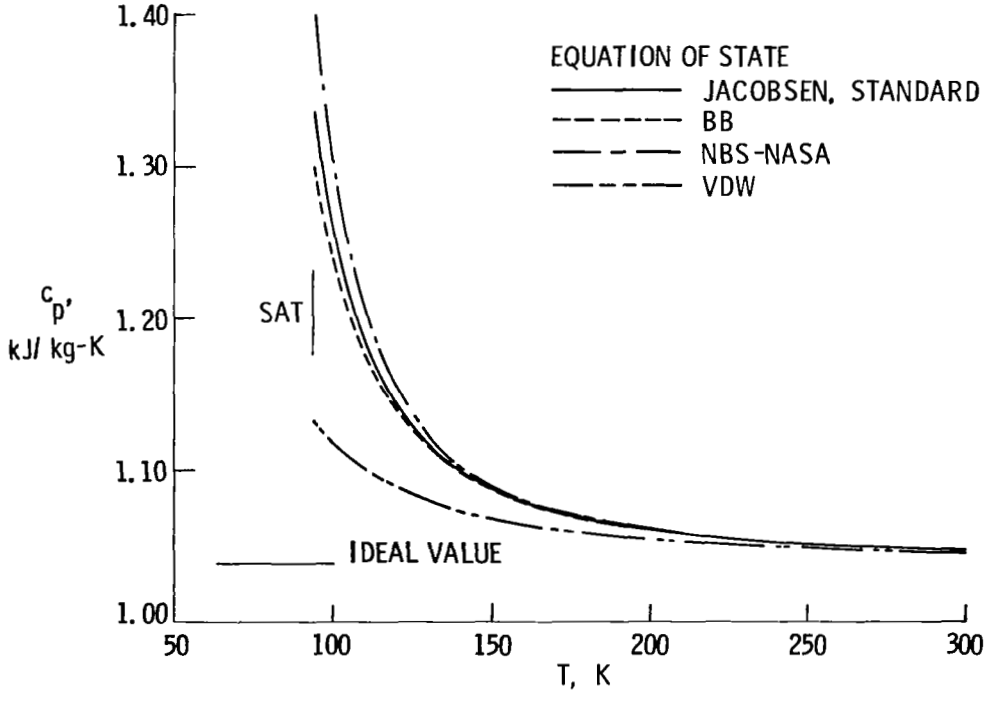

Figure 4.- Specific heat at constant pressure c_p for nitrogen gas at $p = 5$ atm. The Jacobsen curve is taken to be the accepted value.

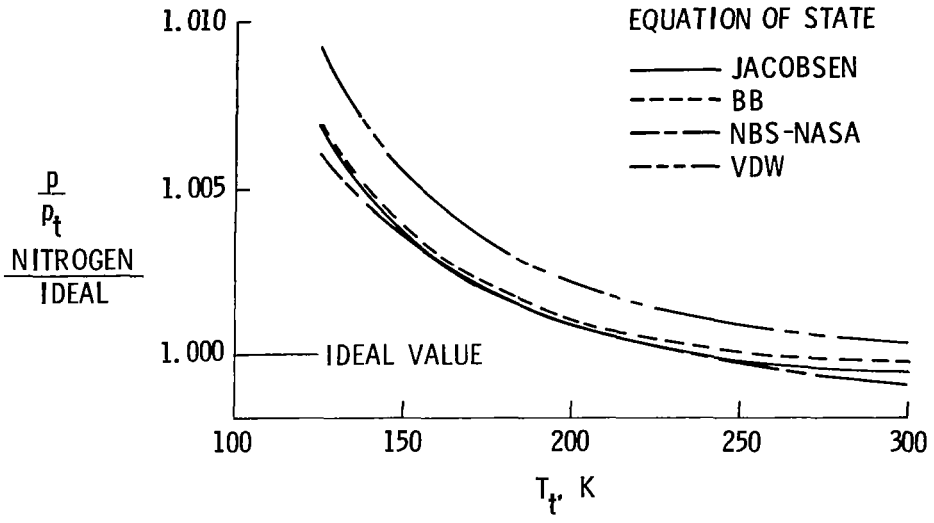

(a) Pressure.

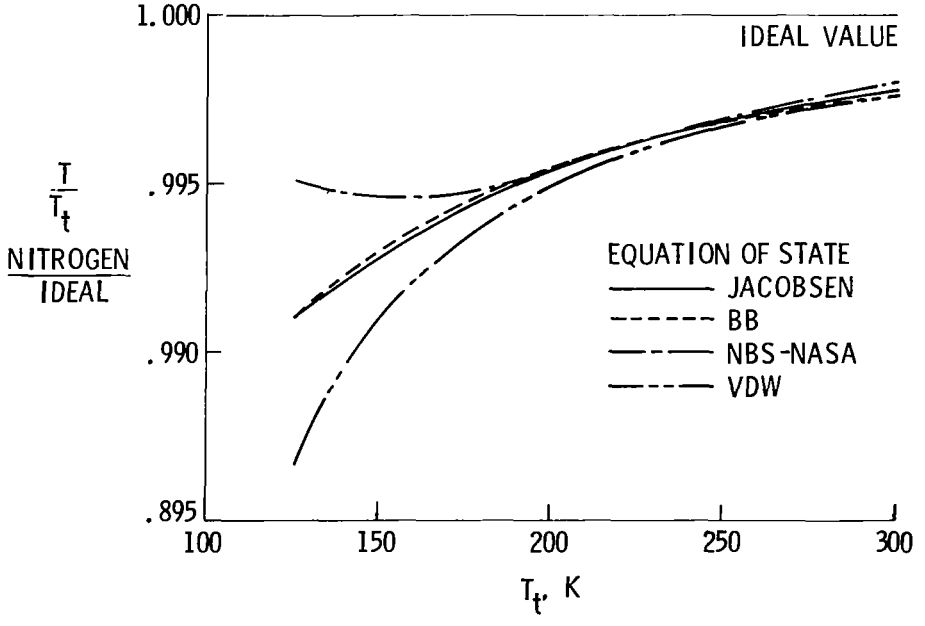

(b) Temperature.

Figure 5.- Isentropic expansion ratios for nitrogen expanded to M = 1.5 at p_t = 9 atm. Ratios normalized by those of an ideal diatomic gas.

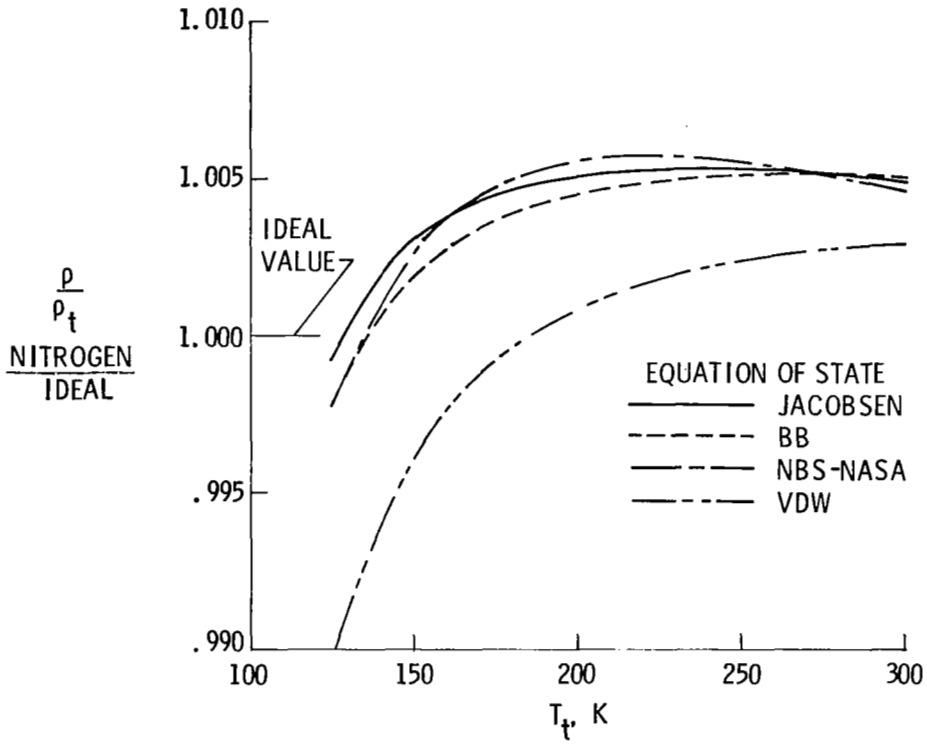

(c) Density.

Figure 5.- Concluded.

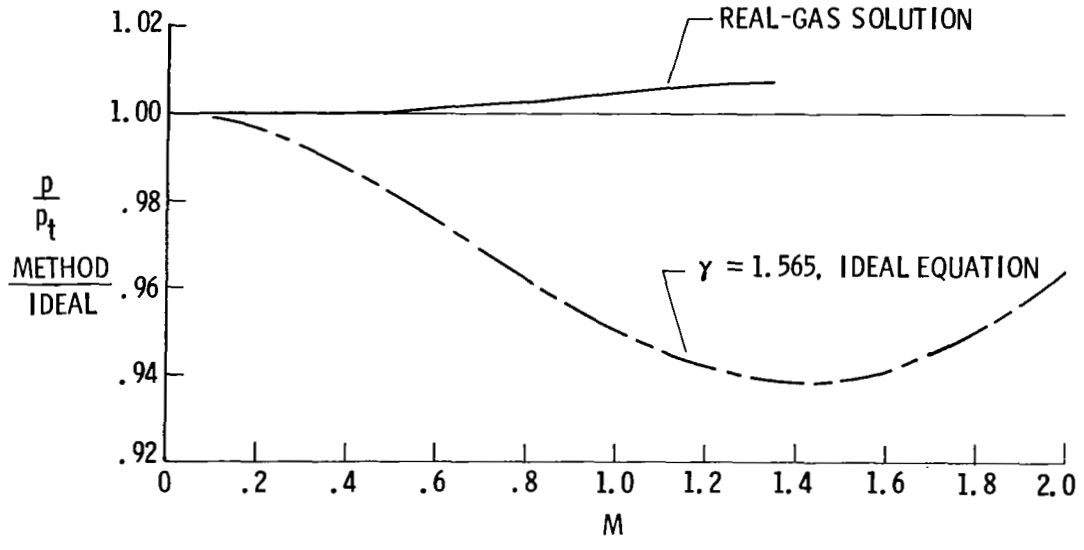

Figure 6.- Isentropic expansion pressure ratios for nitrogen determined by two methods. Ratios normalized by those of an ideal diatomic gas with $\gamma = 1.4$. $p_t = 8$ atm; $T_t = 120$ K. (From ref. 8.)

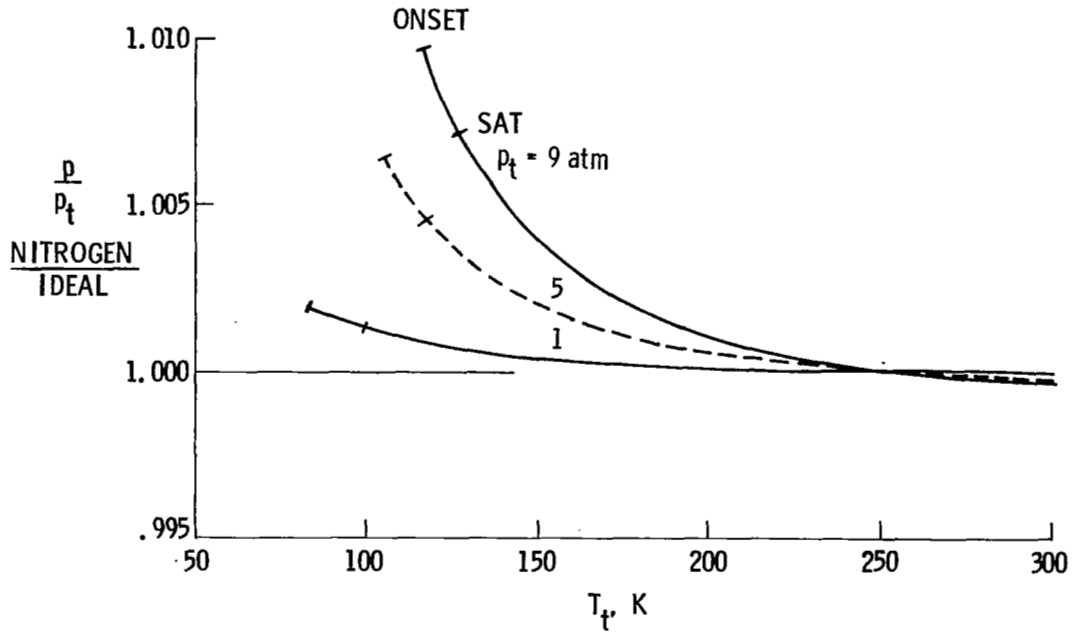

(a) Pressure.

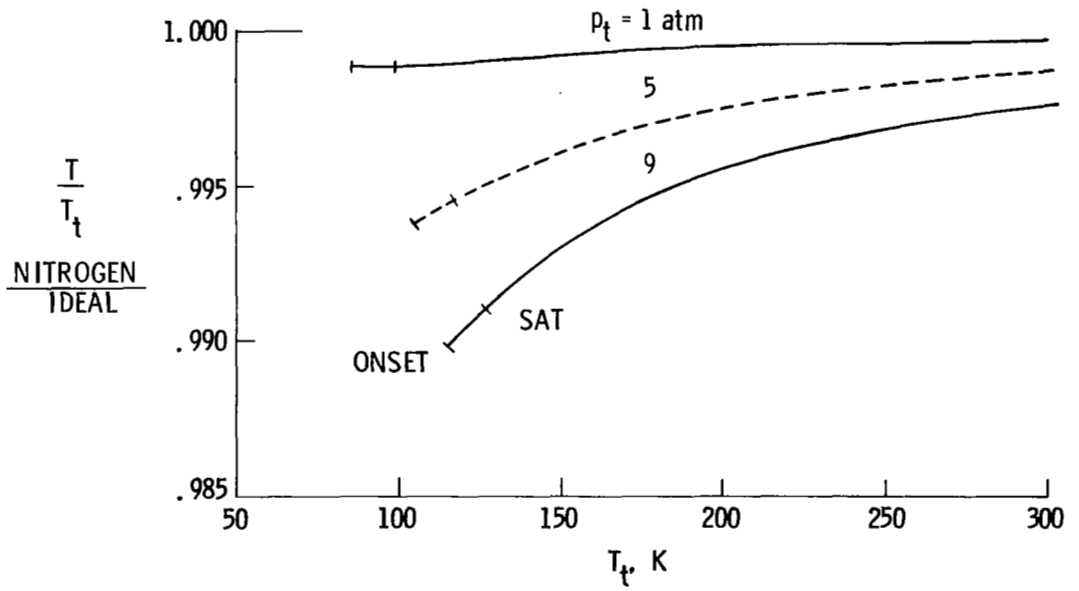

(b) Temperature.

Figure 7.- Isentropic expansion ratios for nitrogen expanded to M = 1.5, calculated using BB equation of state. Ratios normalized by those of an ideal diatomic gas.

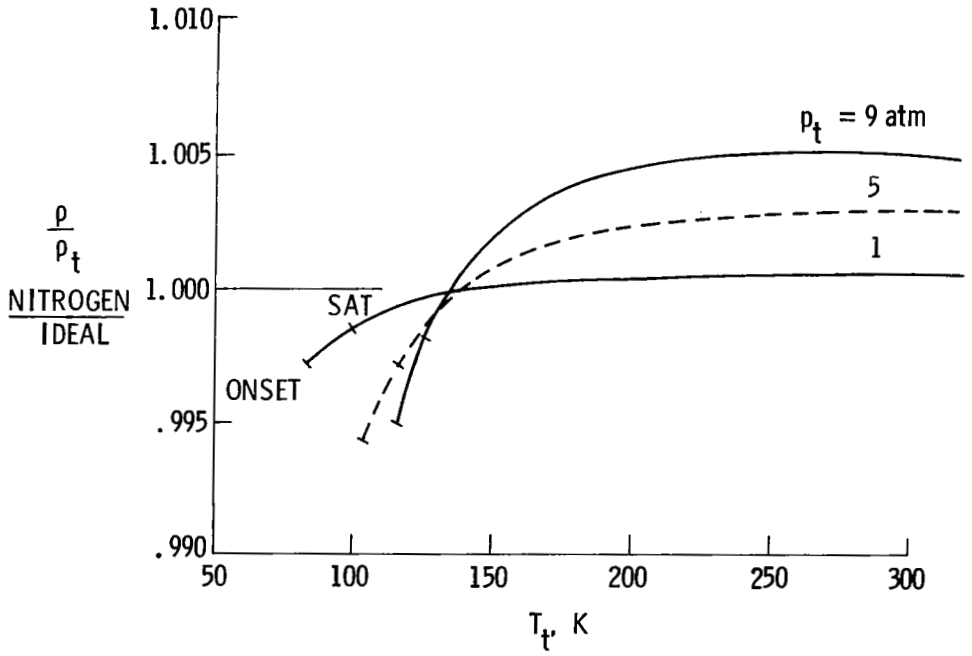

(c) Density.

Figure 7.- Concluded.

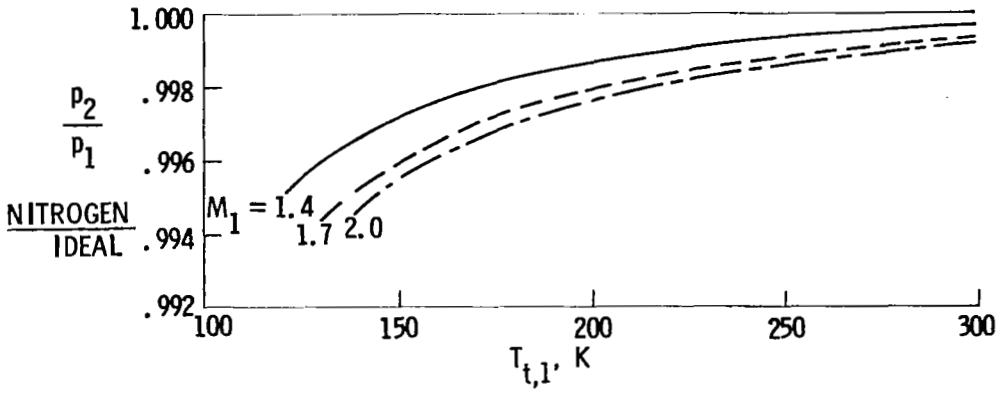

(a) Pressure.

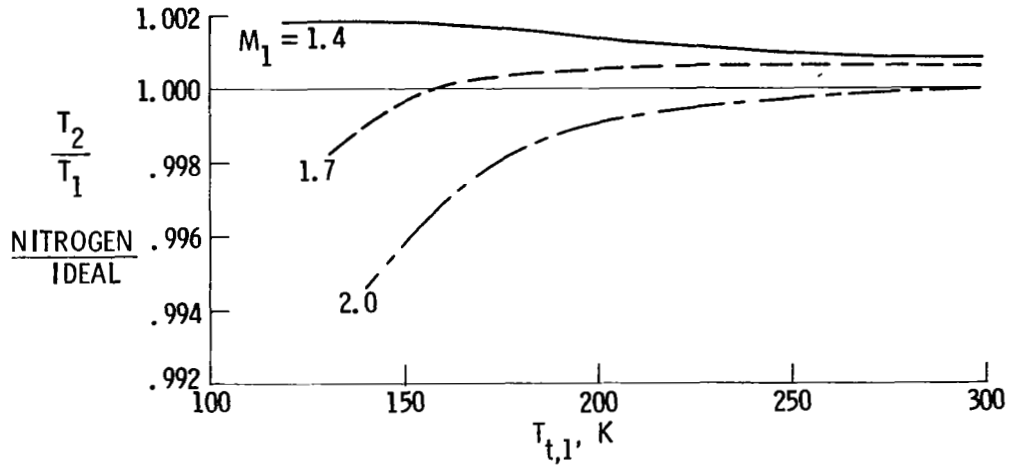

(b) Temperature.

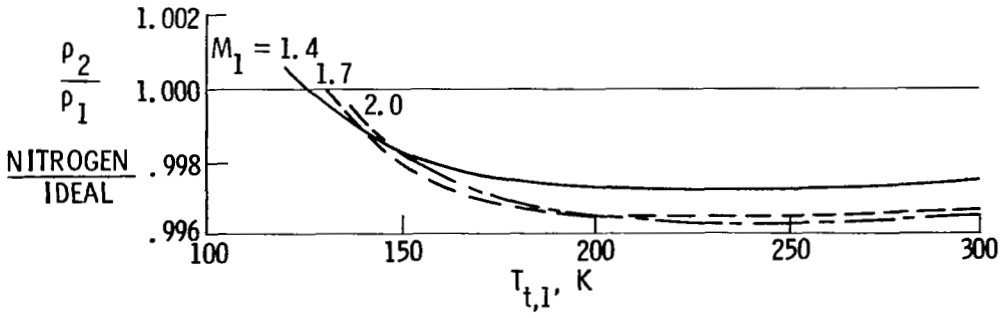

(c) Density.

Figure 8.- Static ratios across a normal shock in nitrogen for various upstream Mach numbers M_1. Ratios normalized by those of an ideal diatomic gas. p_t = 8 atm. (From ref. 8.)

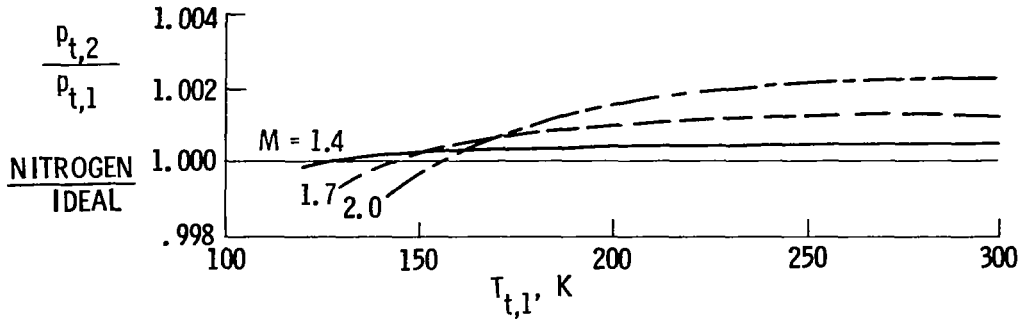

(a) Pressure.

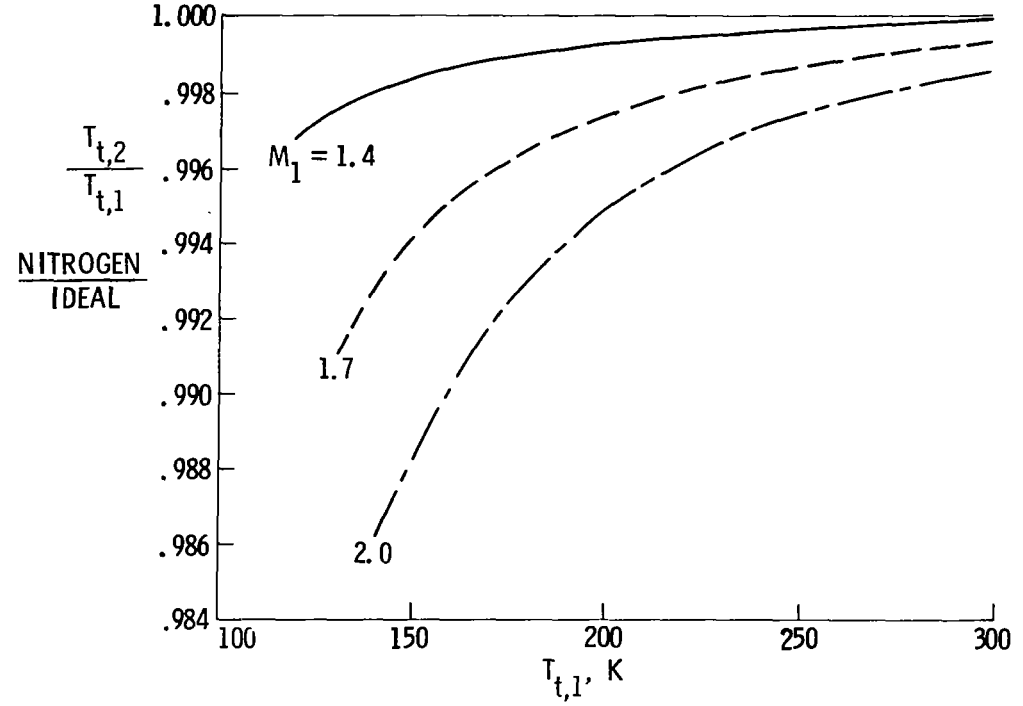

(b) Temperature.

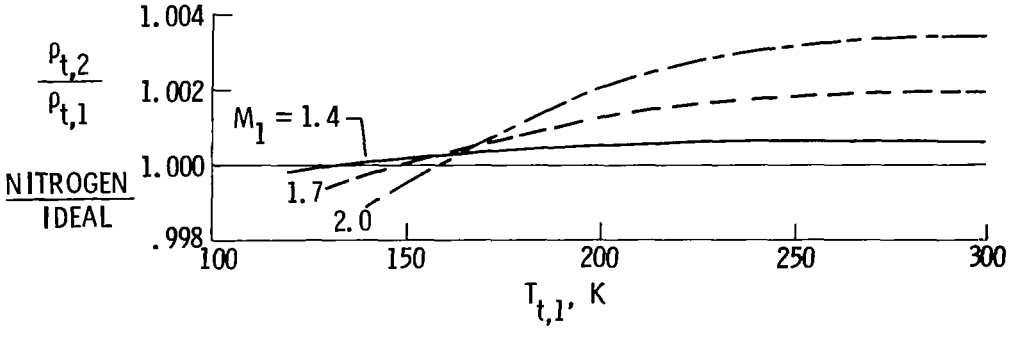

(c) Density.

Figure 9.- Total ratios across a normal shock in nitrogen for various upstream Mach numbers M_1. Ratios normalized by those of an ideal diatomic gas. p_t = 8 atm. (From ref. 8.)

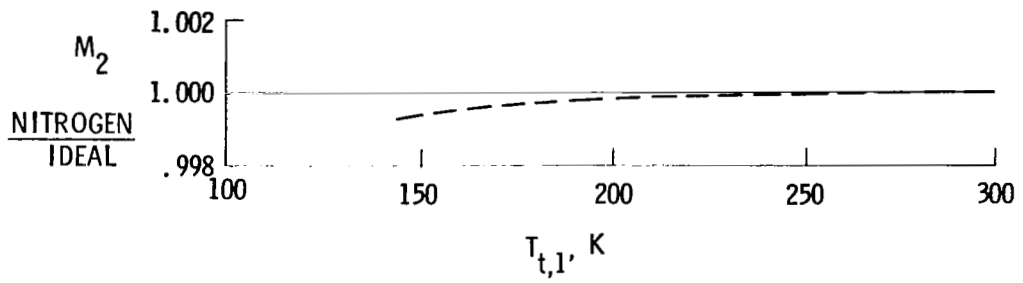

Figure 10.- Mach number downstream of normal shock M_2 in nitrogen. Ratios normalized by those of an ideal diatomic gas. $M_1 = 2.0$; $p_t = 10$ atm. (From ref. 8.)

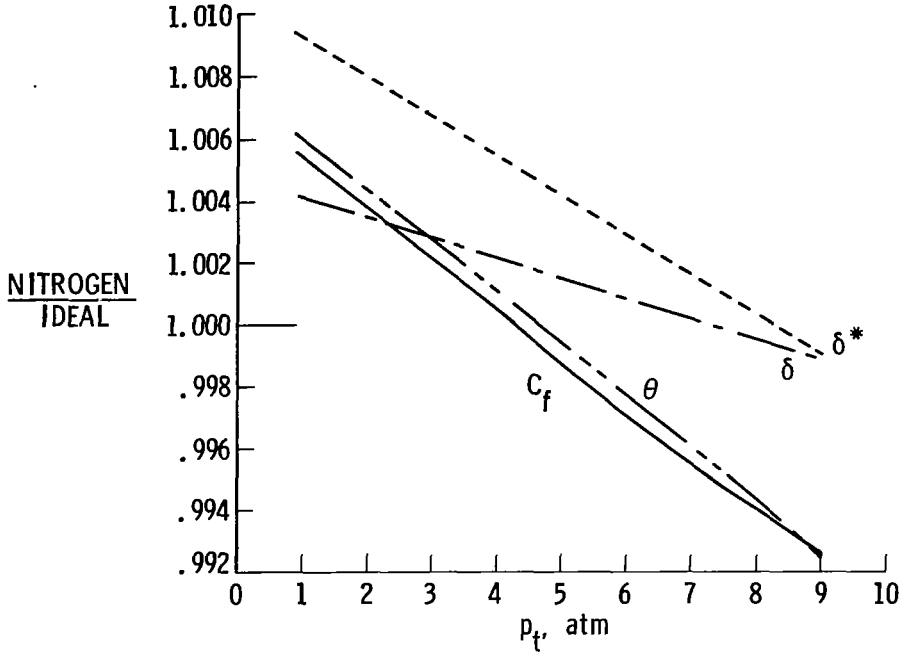

(a) As a function of p_t. $M_\infty = 0.85$; $T_t = 120$ K.

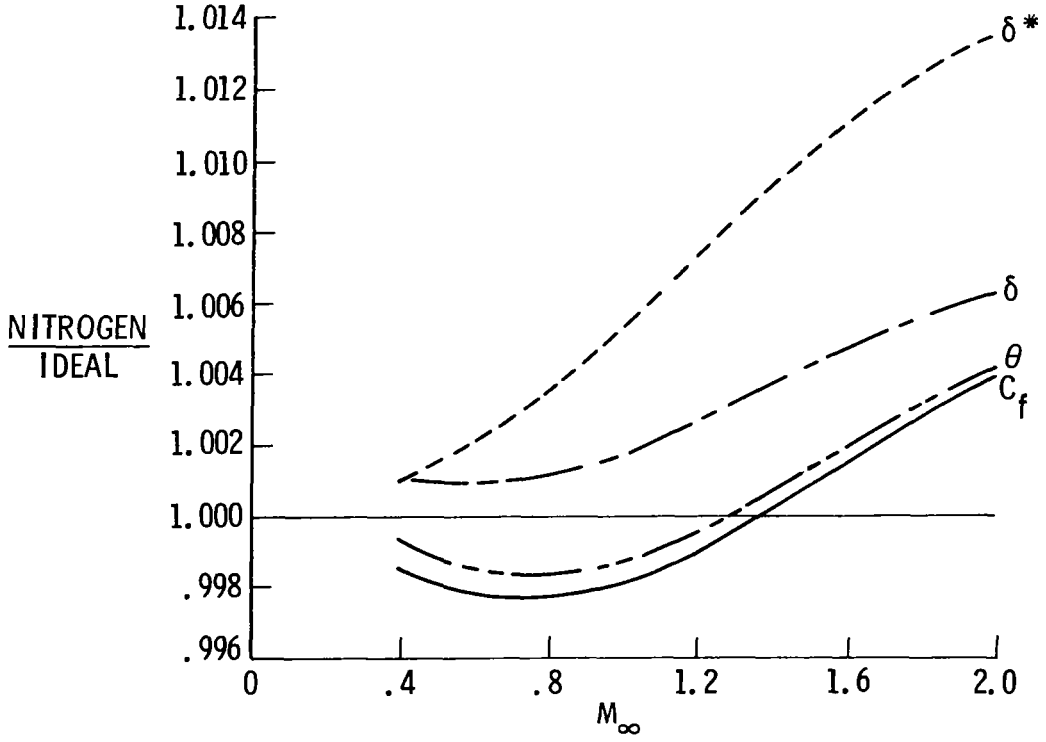

(b) As a function of M_∞. $p_t = 9$ atm; $T_t = 150$ K.

Figure 11.- Parameters for laminar adiabatic-wall boundary layers on a flat plate for nitrogen, relative to ideal values. (From ref. 13.)

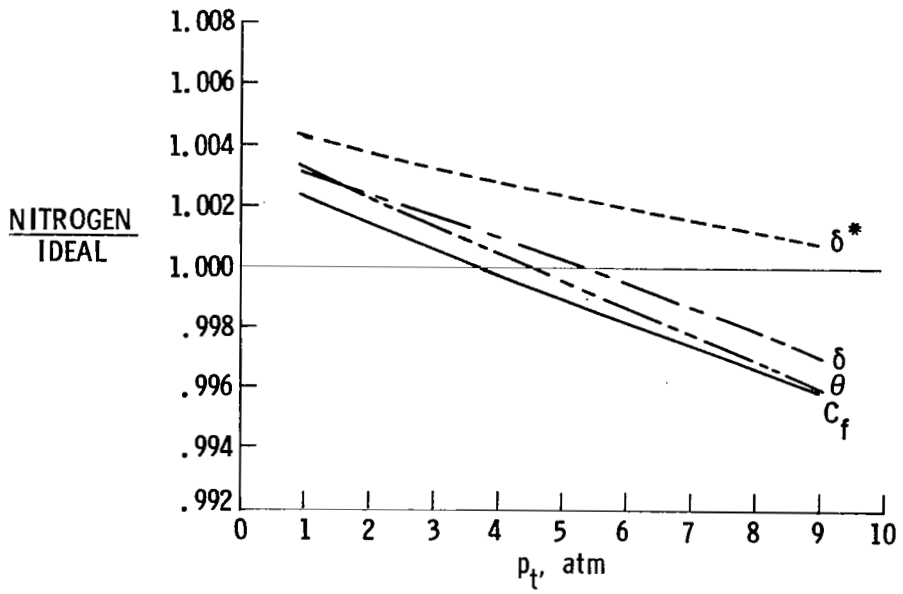

(a) As a function of p_t. $M_\infty = 0.85$; $T_t = 120$ K.

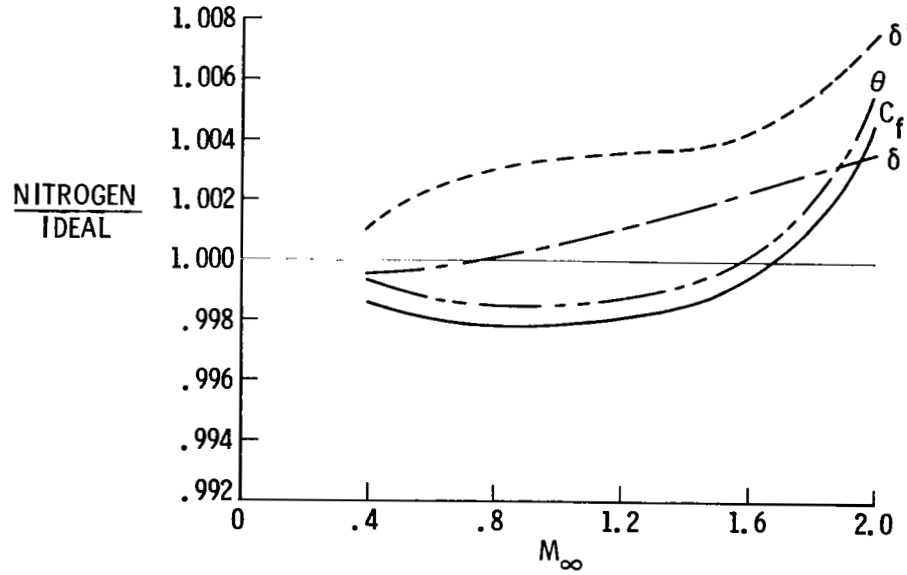

(b) As a function of M_∞. $p_t = 9$ atm; $T_t = 150$ K.

Figure 12.- Parameters for turbulent adiabatic-wall boundary layers on a flat plate for nitrogen, relative to ideal values. (From ref. 13.)

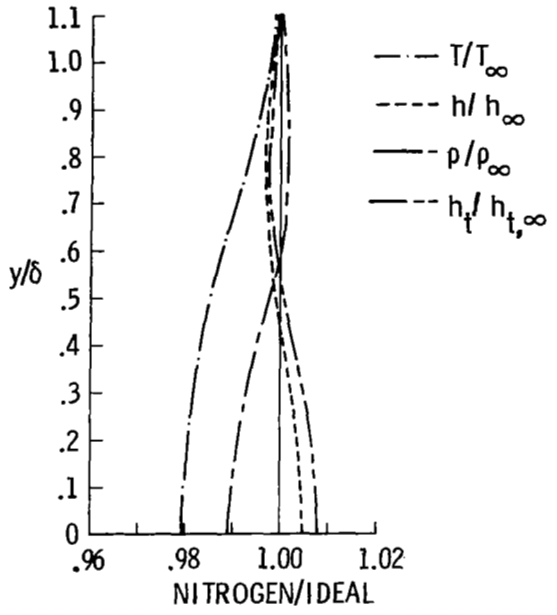

(a) Laminar.

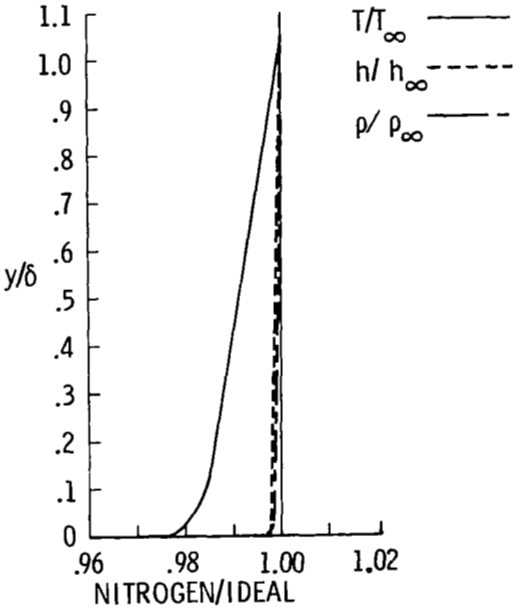

(b) Turbulent.

Figure 13.- Adiabatic profiles for nitrogen flow over a flat plate, relative to ideal values. $M_\infty = 0.85$; $p_t = 9$ atm; $T_t = 120$ K; $R_x = 140 \times 10^6$. (From ref. 13.)

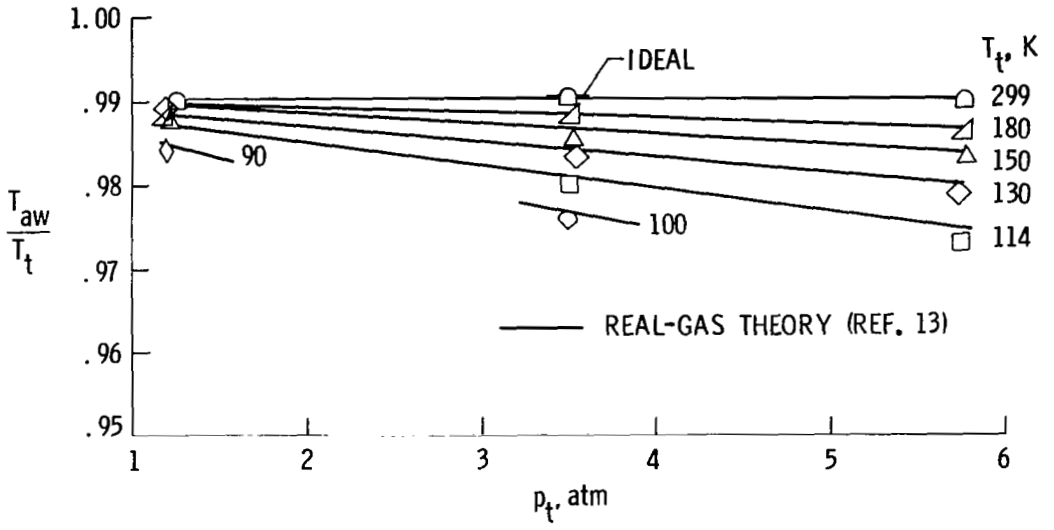

Figure 14.- Adiabatic-wall temperature at a 40% chord location for various stagnation conditions. Data given by symbols. M = 0.70. (From ref. 14.)

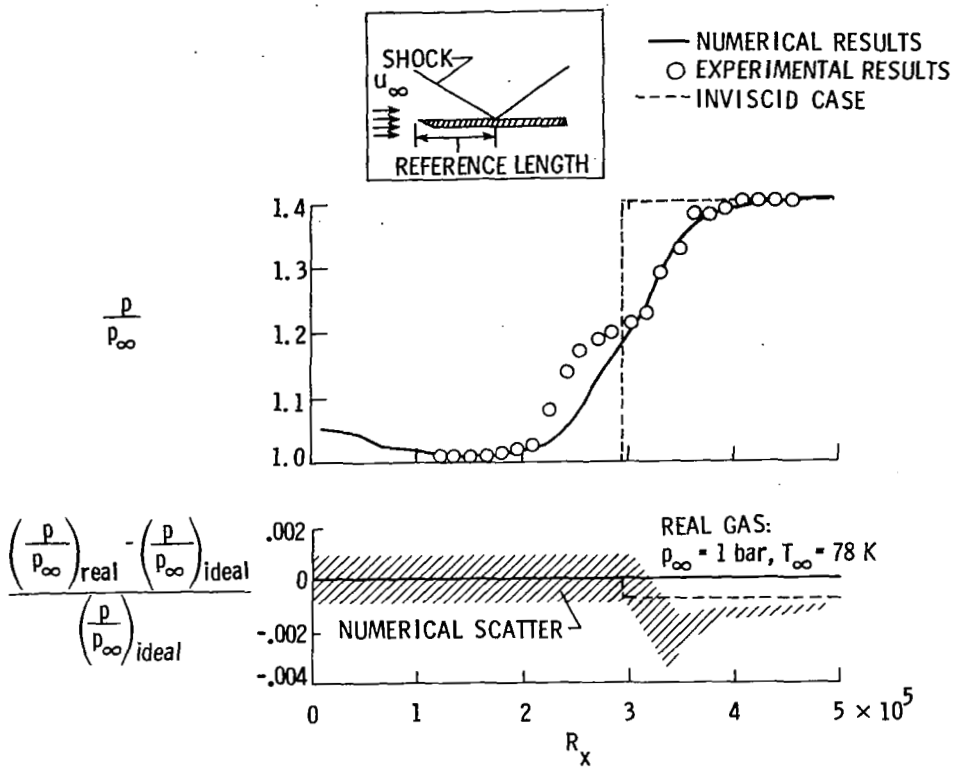

Figure 15.- Pressure distribution for interaction between shock wave and boundary layer. Reynolds number at shock intersection with flat plate, 2.96×10^5; $M_\infty = 2.0$; $\zeta = 32.6°$. (Reprinted with permission of AIAA from ref. 10.)

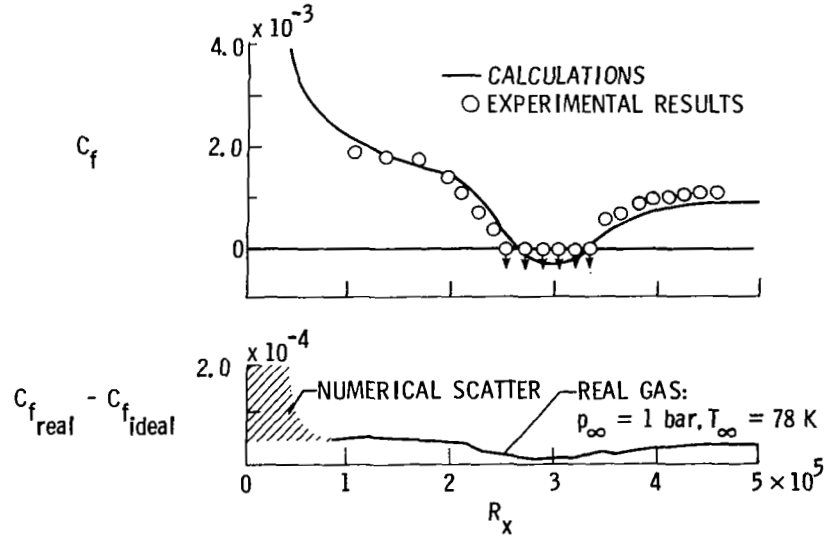

Figure 16.- Skin friction coefficient for interaction between shock wave and boundary layer. Reynolds number at shock intersection with flat plate, 2.96×10^5; $M_\infty = 2.0$; $\zeta = 32.6°$. (Reprinted with permission of AIAA from ref. 10.)

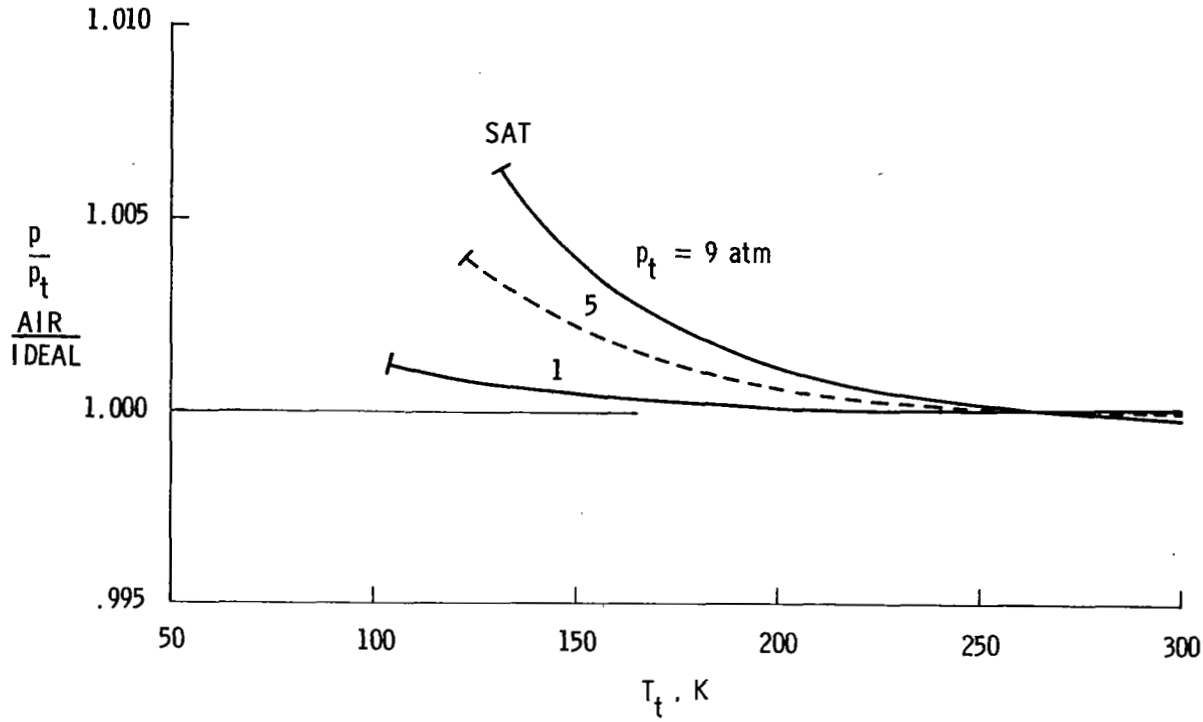

(a) Pressure.

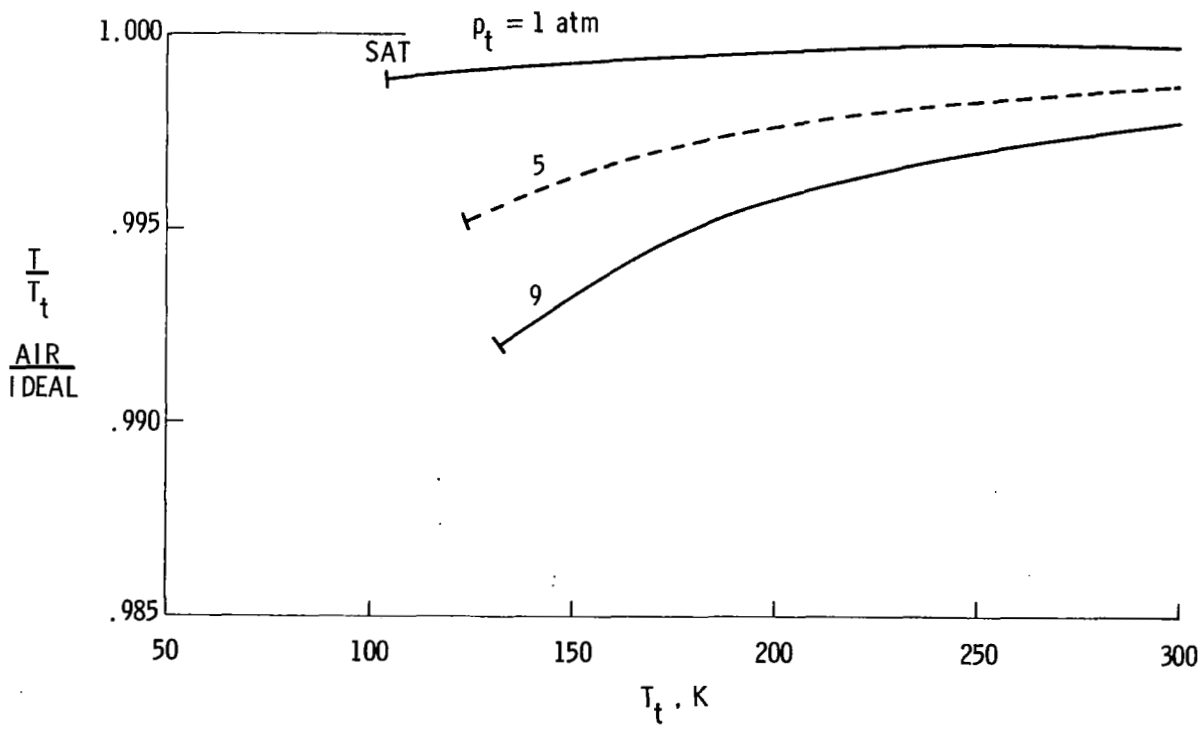

(b) Temperature.

Figure 17.- Isentropic expansion ratios for air expanded to M = 1.5 calculated using BB equation of state. Ratios normalized by those of an ideal diatomic gas.

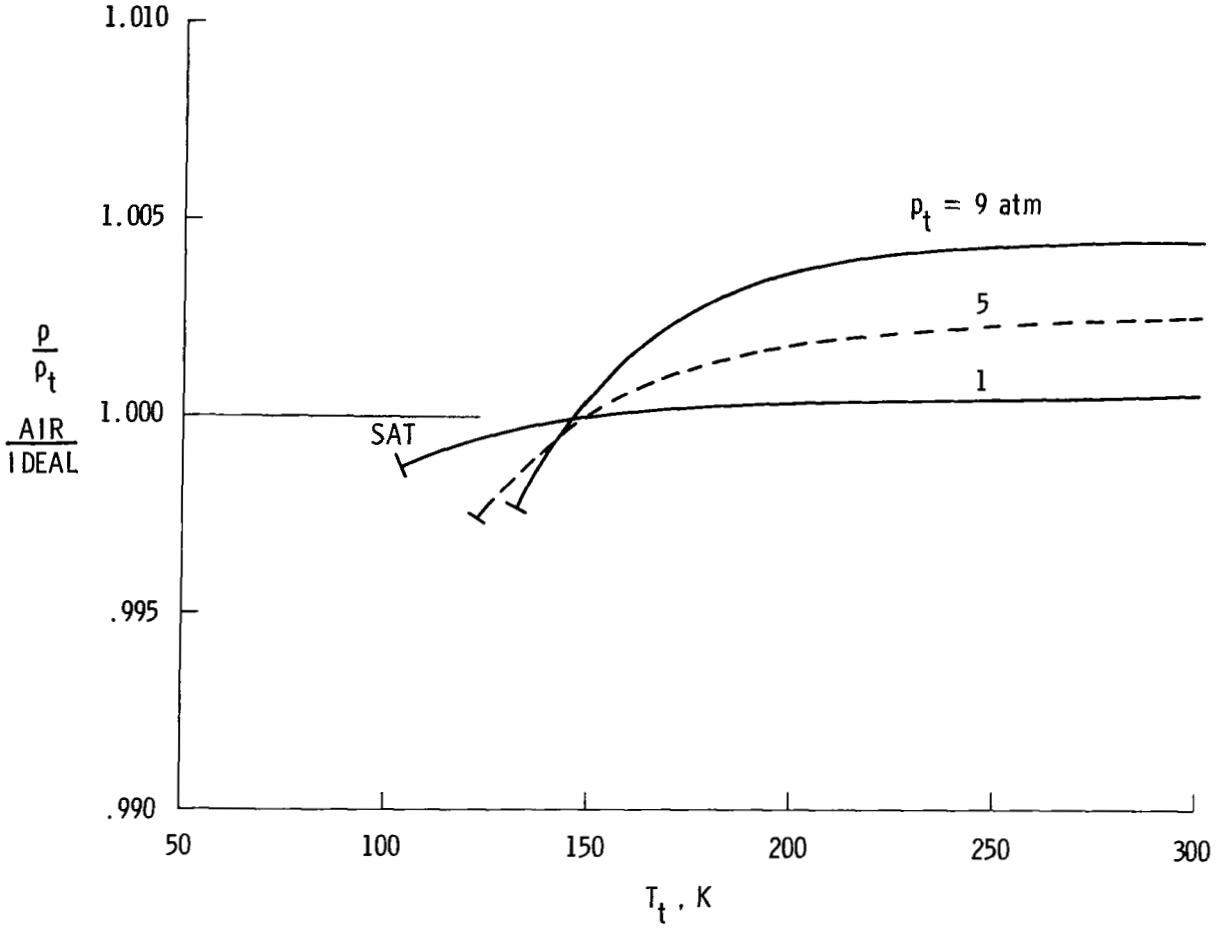

(c) Density.

Figure 17.- Concluded.

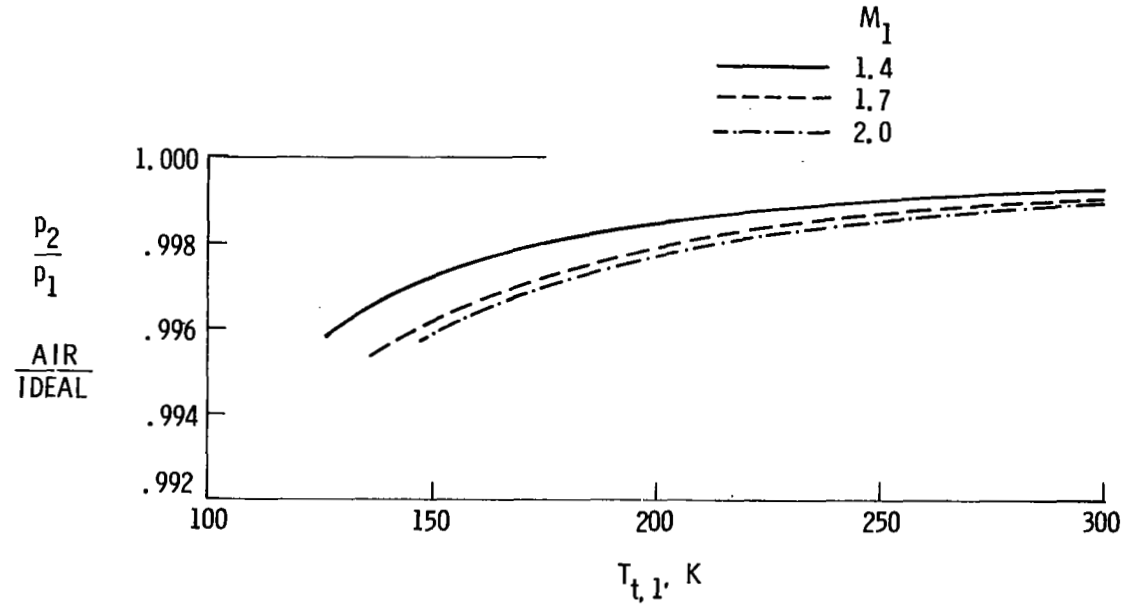

(a) Pressure.

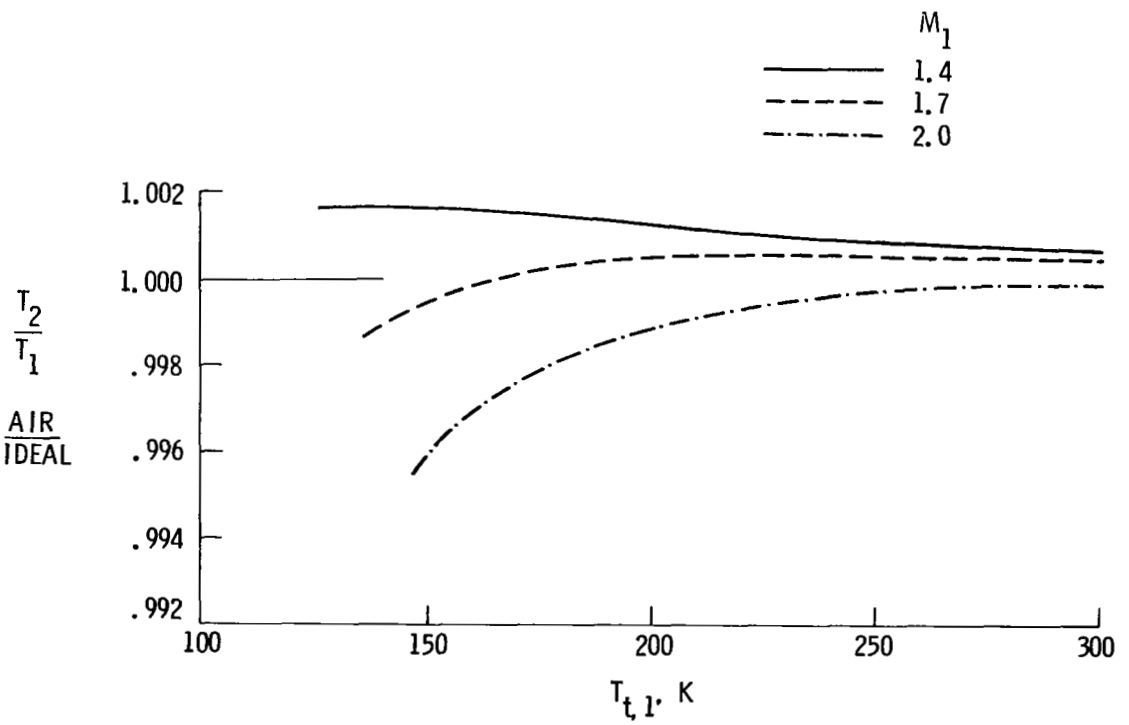

(b) Temperature.

Figure 18.- Static ratios across a normal shock in air for various upstream Mach numbers M_1, calculated using BB equation of state. Ratios normalized by those of an ideal diatomic gas. p_t = 8 atm.

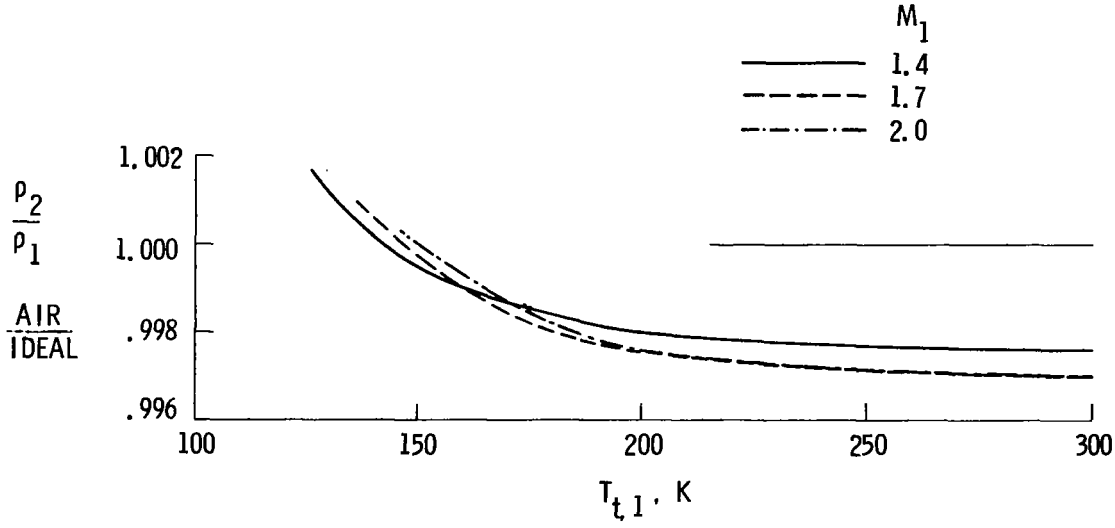

(c) Density.

Figure 18.- Concluded.

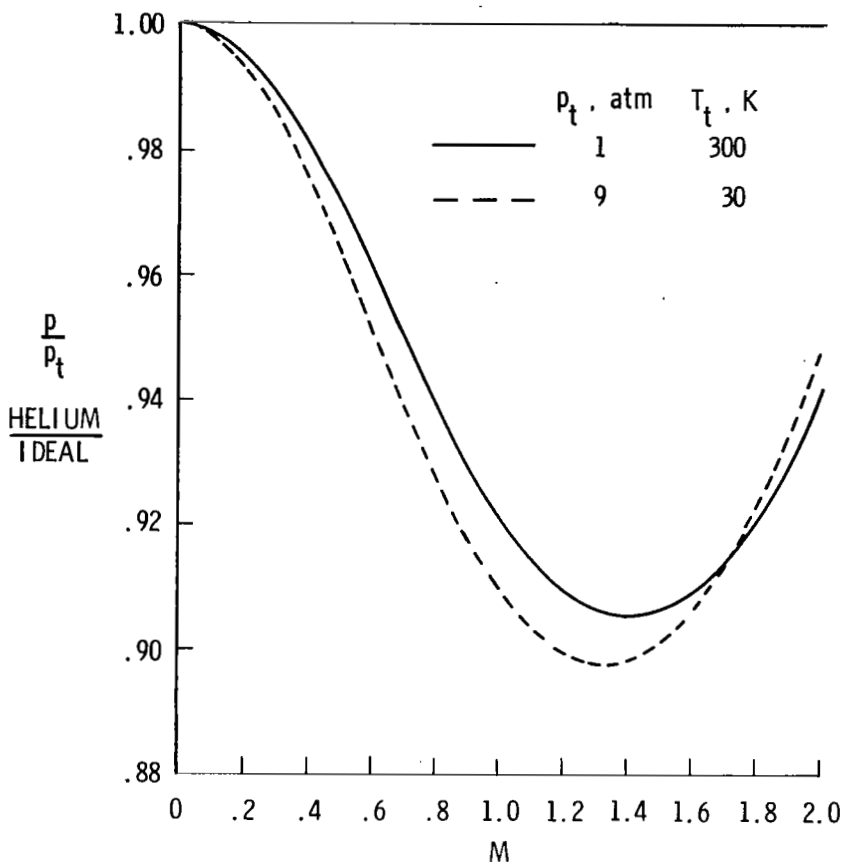

(a) Pressure.

Figure 19.- Isentropic expansion ratios for helium as a function of M, calculated using BB equation of state. Ratios normalized by those of an ideal diatomic gas.

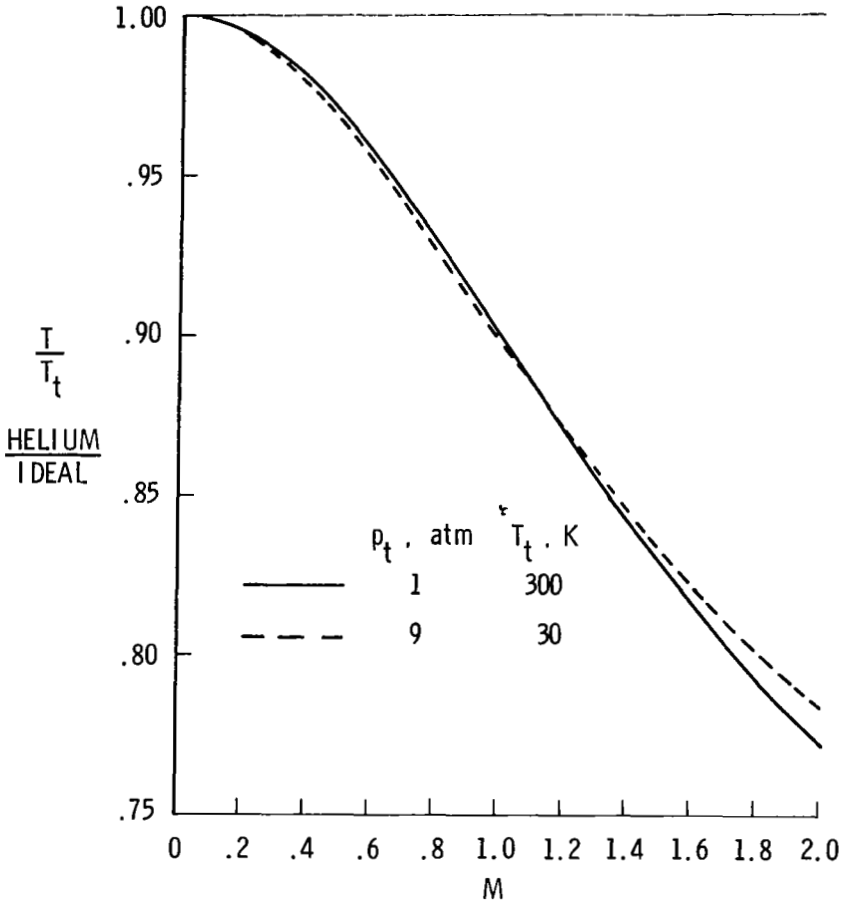

(b) Temperature.

Figure 19.- Continued.

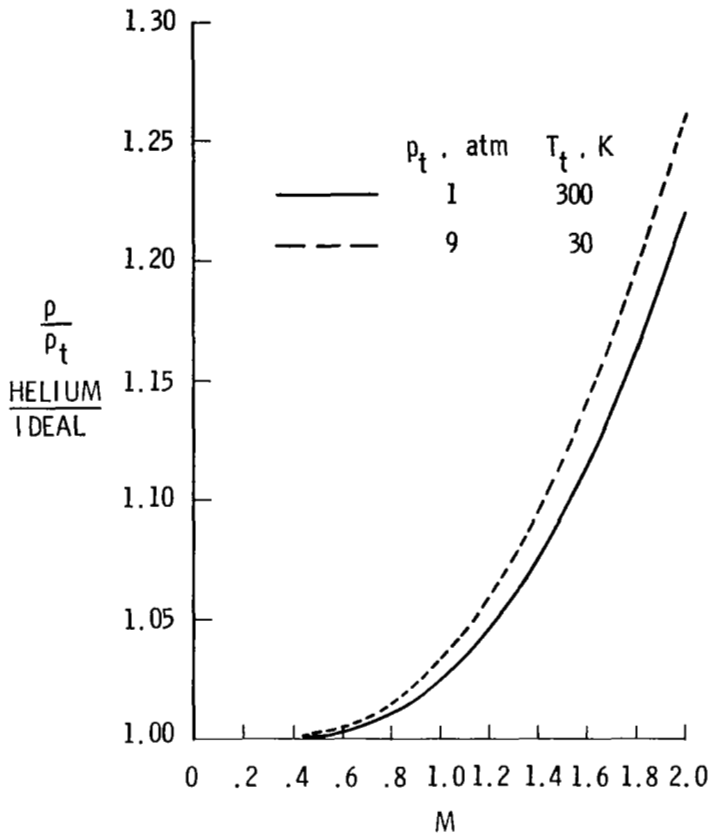

(c) Density.

Figure 19.- Concluded.

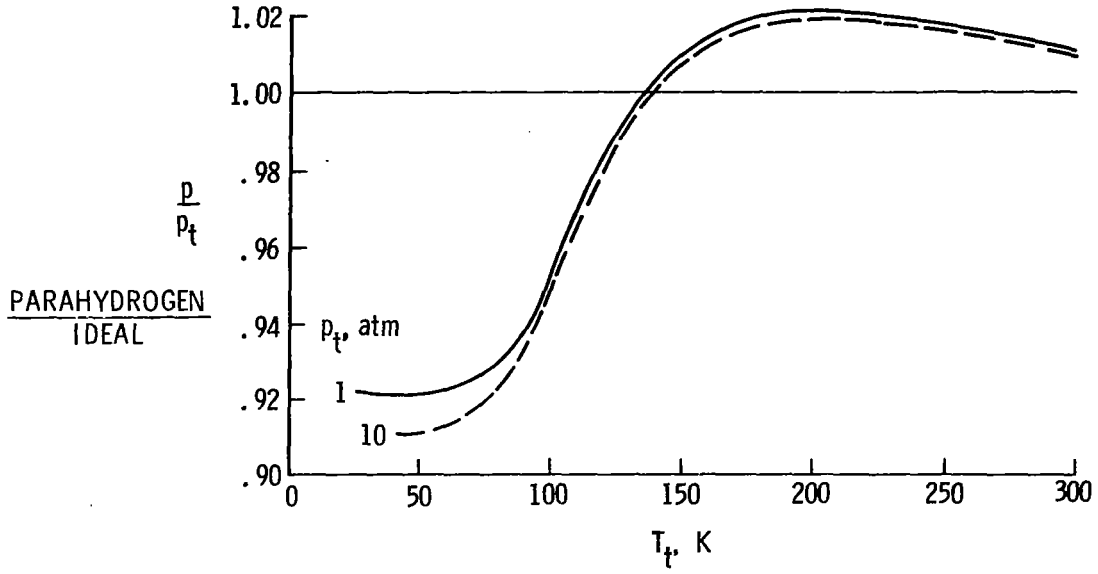

(a) Pressure.

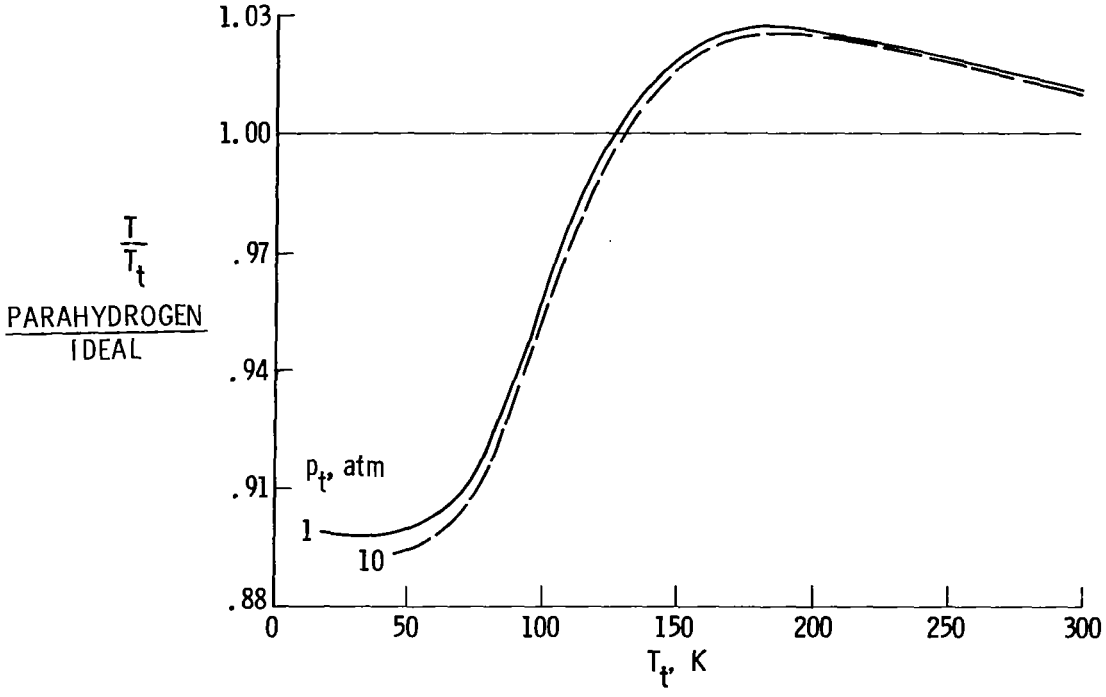

(b) Temperature.

Figure 20.- Isentropic expansion ratios for parahydrogen expanded to M = 1.0. Ratios normalized by those of an ideal diatomic gas. (From ref. 18.)

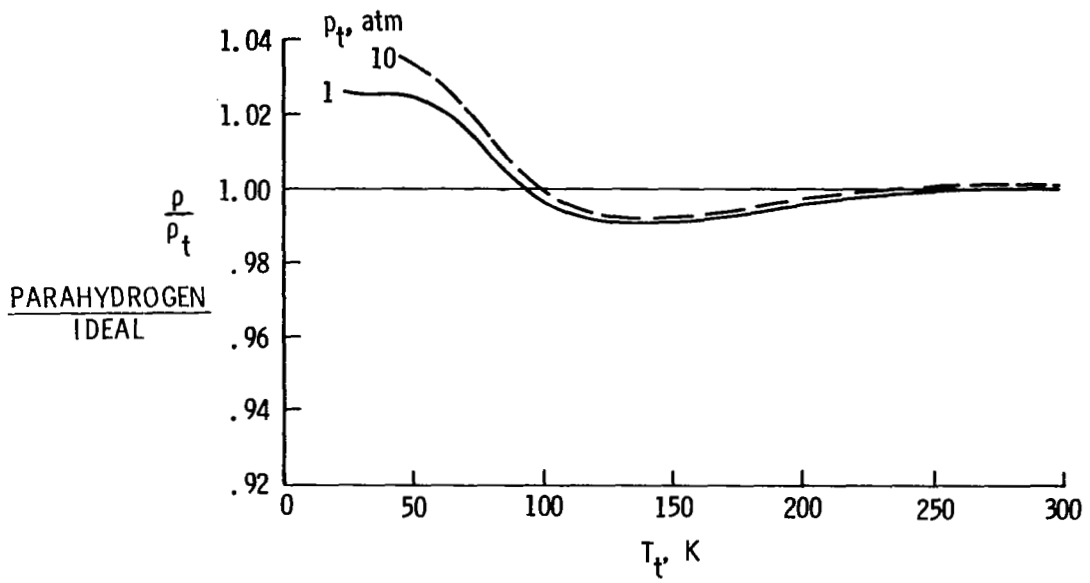

(c) Density.

Figure 20.- Concluded.

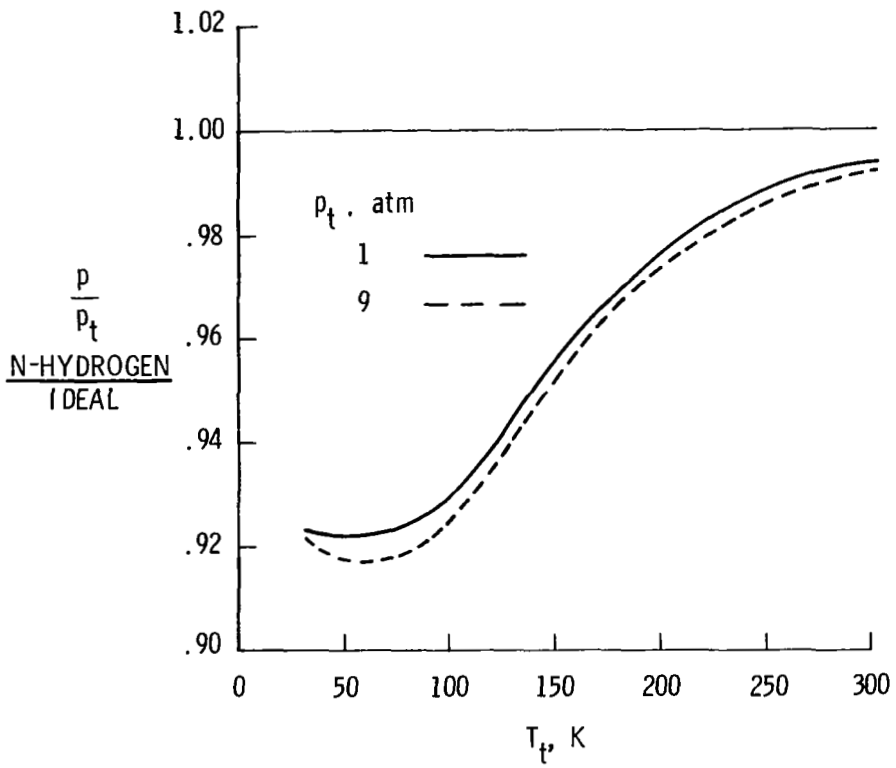

(a) Pressure.

Figure 21.- Isentropic expansion ratios for n-hydrogen expanded to M = 1.0 assuming that BB equation of state applies and using n-hydrogen values for c_{p_0}. Ratios normalized by those of an ideal diatomic gas.

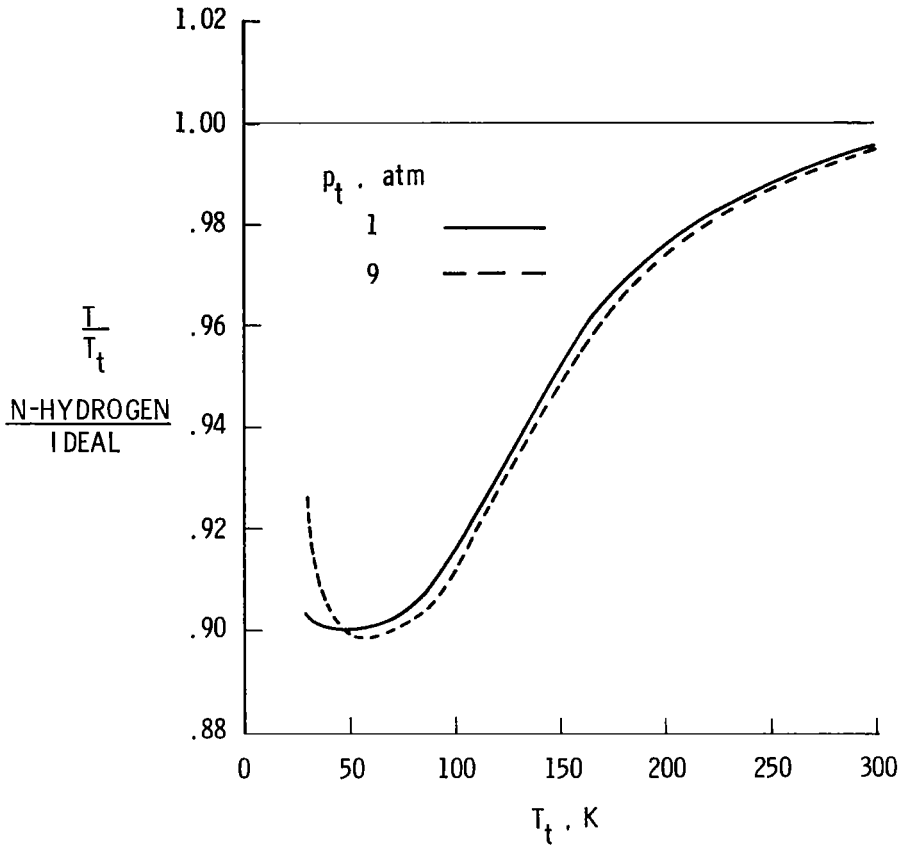

(b) Temperature.

Figure 21.- Continued.

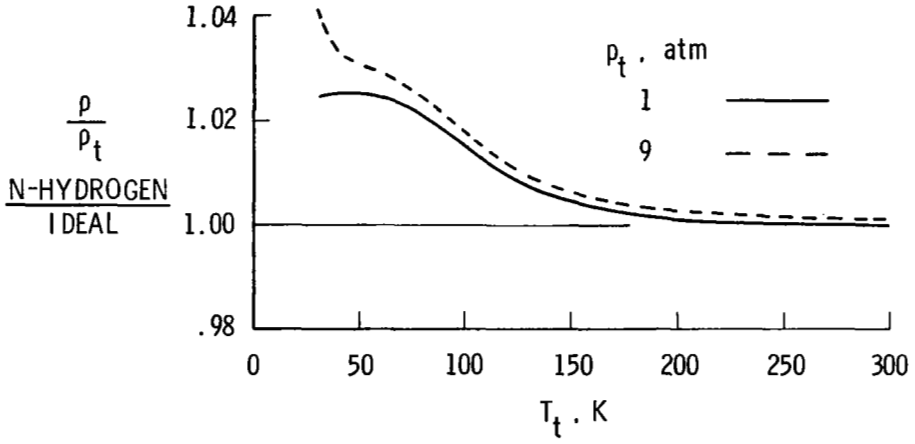

(c) Density.

Figure 21.- Concluded.

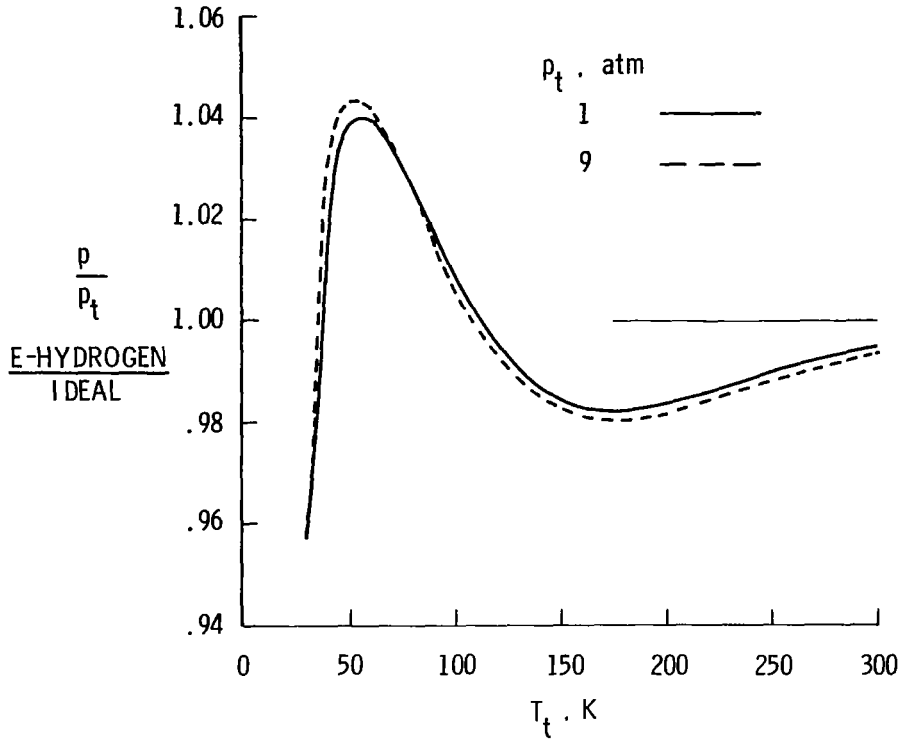

(a) Pressure.

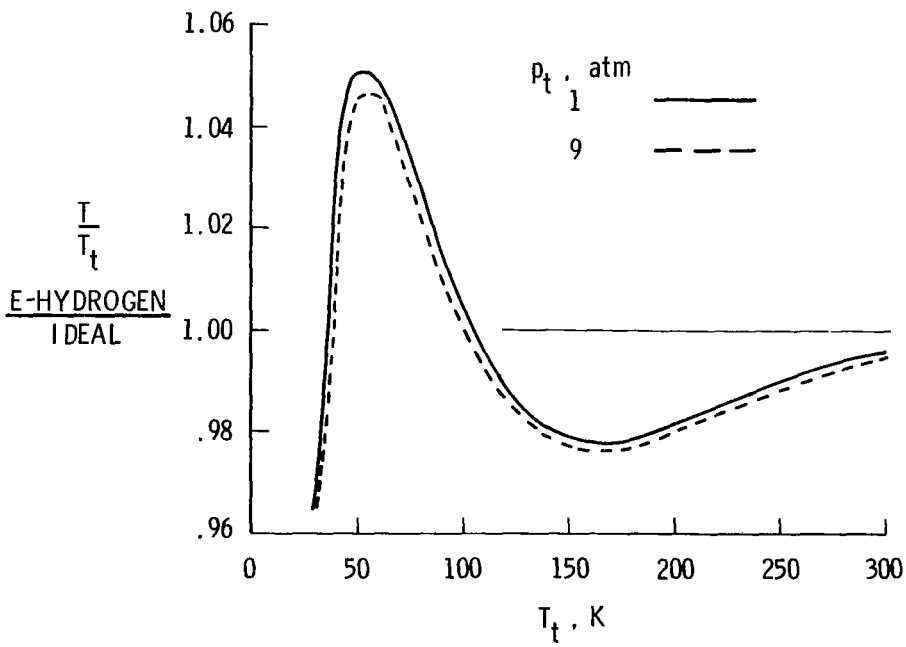

(b) Temperature.

Figure 22.- Isentropic expansion ratios for e-hydrogen expanded to M = 1.0 assuming that BB equation of state applies and using e-hydrogen values for c_{p_0}. Ratios normalized by those of an ideal diatomic gas.

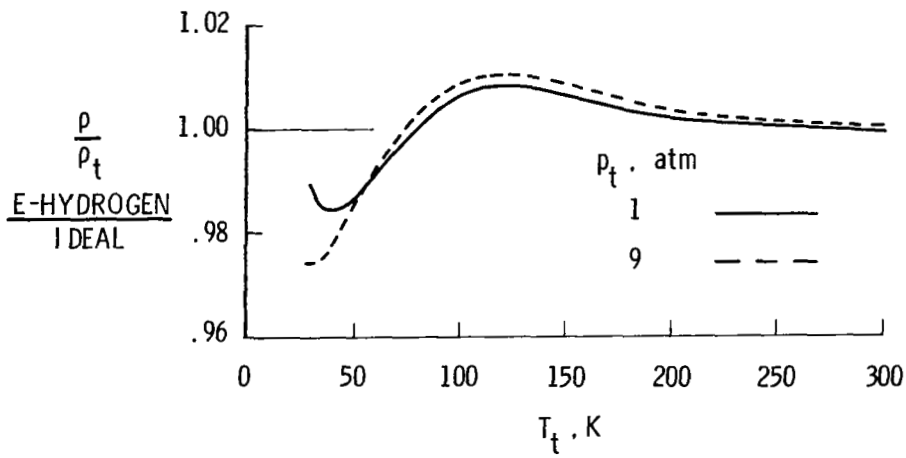

(c) Density.

Figure 22.- Concluded.

1. Report No.	2. Government Accession No.	3. Recipient's Catalog No.
NASA TP-1901		

4. Title and Subtitle	5. Report Date
SIMULATION OF IDEAL-GAS FLOW BY NITROGEN AND OTHER SELECTED GASES AT CRYOGENIC TEMPERATURES	September 1981
	6. Performing Organization Code: 505-31-53-01
7. Author(s): Robert M. Hall and Jerry B. Adcock	8. Performing Organization Report No.: L-14587
	10. Work Unit No.
9. Performing Organization Name and Address: NASA Langley Research Center, Hampton, VA 23665	11. Contract or Grant No.
	13. Type of Report and Period Covered: Technical Paper
12. Sponsoring Agency Name and Address: National Aeronautics and Space Administration, Washington, DC 20546	14. Sponsoring Agency Code

15. Supplementary Notes

16. Abstract

Cooling the test gas in a transonic wind tunnel to cryogenic temperatures can very effectively increase Reynolds number without increasing model loads. However, the flow of gases at cryogenic temperatures may significantly depart from that of an ideal diatomic gas representative of most transonic flight. Consequently, the real-gas behavior of nitrogen, the gas normally used in transonic cryogenic tunnels, is reported for the following flow processes: isentropic expansion, normal shocks, boundary layers, and interactions between shock waves and boundary layers. The only differences in predicted pressure ratio between nitrogen and an ideal gas which may limit the minimum operating temperatures of transonic cryogenic wind tunnels occur at total pressures approaching 9 atm and total temperatures 10 K below the corresponding saturation temperature. These pressure differences approach 1 percent for both isentropic expansions and normal shocks. Several alternative cryogenic test gases - dry air, helium, and hydrogen - are also analyzed. Differences between air and an ideal diatomic gas are similar in magnitude to those for nitrogen and should present no difficulty. However, differences for helium and hydrogen are over an order of magnitude greater than those for nitrogen or air. It is concluded that helium and cryogenic hydrogen would not approximate the compressible flow of an ideal diatomic gas.

17. Key Words (Suggested by Author(s))	18. Distribution Statement
Cryogenic wind tunnel Real-gas effects Transonic flow simulation Nitrogen Air Hydrogen Helium	Unclassified - Unlimited Subject Category 34

19. Security Classif. (of this report)	20. Security Classif. (of this page)	21. No. of Pages	22. Price
Unclassified	Unclassifed	49	A03

For sale by the National Technical Information Service, Springfield, Virginia 22161

NASA-Langley, 1981